ADVANCED POLYMER/COMPOSITE MATERIAL MODELING FOR AUTOMOTIVE APPLICATIONS

EVALUATION OF STRUCTURAL COUNTERMEASURES FOR NHTSA'S OBLIQUE FRONTAL IMPACT

MARCH 1, 2019

PREPARED BY

R REICHERT, CK PARK, AND CD KAN

CENTER FOR COLLISION AND SAFETY ANALYSIS

GEORGE MASON UNIVERSITY

WILLIAM THOMAS HOLLOWELL

WTH CONSULTING LLC

SUBMITTED TO

AMERICAN CHEMISTRY COUNCIL

Contact information

Dr. William Thomas Hollowell
E-mail: Tom.Hollowell@WTHConsulting.com

WTH Consulting LLC
2634 Iveysprings Court,
Apex, NC 27539, USA

Rudolf Reichert
E-mail: reichert@gmu.edu

Dr. CK Park
E-mail: ckpark@gmu.edu

Dr. Steve Kan
E-mail: cdkan@gmu.edu

Center for Collision Safety and Analysis (CCSA)
George Mason University
4087 University Drive, Suite 2100 (MSN:6B8)
Fairfax, VA 22030, USA
https://www.ccsa.gmu.edu/

Executive Summary

The George Mason University (GMU) was commissioned by the American Chemistry Council (ACC) to conduct research to understand numerical polymer/composite material models and their computer-aided engineering (CAE) applications. Research documented in this report demonstrate the light-weighting opportunity of composites in structural components of a vehicle, and are in line with the 'ACC's Plastics and Polymer Composites Technology Roadmap for Automotive Markets.'

Crash test results have shown that vehicles may require structural modifications for good performance in NHTSA's frontal oblique test procedure. In a previous project, funded by NHTSA, the GMU Team determined incremental vehicle structural change requirements using steel materials and their associated mass to significantly reduce occupant compartment intrusion. A finite element (FE) model of a mid-size sedan was updated and validated using data from a 2015 Toyota Camry. The generated baseline model correlated well with oblique and co-linear crash configurations. An iterative process was used to develop structural countermeasures to reduce occupant compartment intrusion for the left and right oblique impact configuration. No unintended consequences, i.e. no considerable increase of vehicle pulse for oblique and co-linear load cases were observed. The associated added mass to reduce intrusion by at least 60% was +17 kg using high-strength steel materials.

The previously developed FE model and tools were used to determine, if similar results, i.e. (1) similar reduction in occupant compartment intrusion, and (2) no unintended consequences, such as significantly more severe vehicle pulses, can be achieved using composite materials for select components.

A similar reduction in occupant compartment intrusion without unintended consequences was achieved. Instead of adding +17 kg of mass when using countermeasures made out of high strength steel materials, it was possible to lightweight the vehicle by -7 kg when using countermeasures made out of composite materials while achieving similar crash characteristics.

As a second pillar of this project, efforts were started in cooperation with Honda and LSTC to develop and validate an advanced composite material model using shell elements. It is anticipated that the new techniques will benefit future research activities of the American Chemistry Council and their members.

Acknowledgements

This research was sponsored by the American Chemistry Council Plastics Division (ACC PD). The authors would like to acknowledge the support of ACC PD and Gina Oliver, Senior Director of ACC PD.

(BLANK)

Table of Contents

List of Figures

List of Tables

(BLANK)

1. Introduction

In fiscal year 2006, Congress directed the National Highway Traffic Safety Administration (NHTSA) of the U.S. Department of Transportation (DOT) to begin the development of a program to examine the possible safety benefits of lightweight Plastics- and Composite-Intensive Vehicles (PCIVs). NHTSA tasked the Volpe National Transportation Systems Center to conduct focused research in cooperation with industry partners from the American Plastics Council (APC), now the American Chemistry Council Plastics Division (ACC-PD).

NHTSA concentrated on the safety-related research issues affecting the deployment of PCIVs in 2020. In 2007, the Volpe Center developed a safety roadmap for future PCIVs and described the approach, activities, and results of an evaluation of potential safety benefits of PCIVs [Brecher 2007, 2009]. Barnes et al. identified outstanding safety issues and research needs for PCIVs to facilitate their safety deployment by 2020, and recommended three topics pertinent to crashworthiness of PCIVs: (1) material database, (2) crashworthiness test method development, and (3) crash modeling [Barnes 2010].

In 2001, the APC (now the ACC-PD) outlined a Vision and Technology Roadmap for the automotive and plastics industries [Fisher 2002]. In the technology integration workshop in 2005, the ACC-PD provided an expansive safety road mapping effort, examining PCIVs [Fisher 2007]. In 2009, the ACC-PD updated the vision and technology roadmap to outline the industry's action priorities for achieving the technology and manufacturing innovations required to realize PCIVs [ACC-PD 2009b]. In addition, the ACC-PD recommended three research activities: (1) improvement of the understanding of composite component response in vehicle crashes, (2) development of a database of relevant parameters for composite materials, and (3) enhancement of predictive models to avoid costly overdesign [ACC-PD 2009a].

There is an increasing need to investigate opportunities for weight reduction of the vehicle fleet to improve fuel economy and compatibility. However, this should be achieved without sacrificing the current self-protection. Innovative plastics and fiber-reinforced composite materials offer a means to lightweight vehicle structures. The main advantages of composites over the more conventional isotropic materials are the lower density, very high specific strength, and specific stiffness that can be achieved.

In 2014, ACC-PD updated the Plastics and Polymer Composites Technology Roadmap for Automotive Markets [ACC-PD 2014] in response to the U.S. Corporate Average Fuel Economy (CAFE) standards in order to develop an effective industry-wide strategy that will extend to 2030 and beyond. The roadmap addresses current barriers and key initiatives to recognize plastics and polymer composites as preferred material solutions that meet automotive performance and sustainability requirements.

As part of implementing the ACC roadmap, ACC partnered with the George Mason University Center for Collision and Safety Analysis (GMU/CCSA) to conduct research to evaluate the application of plastics and composites using Computer-Aided Engineering (CAE) simulations. In a previous, the GMU Team developed a lightweight vehicle by replacing existing steel components with plastics or composite components in a reverse-engineered computer model. To support realistic development, industry partners participated in the project by providing available plastics/composite materials and their application and design. The crashworthiness of the light-weighted components was investigated through impact simulations, both at a component level and at a full vehicle level. The results were documented in [Park, 2017].

A more specific research task was adopted in the current project. Using computer simulation, an evaluation was undertaken to determine if countermeasures using CFRP Modified Automotive Structures in NHTSA's new frontal oblique impact test can achieve similar reduction in occupant compartment intrusion as countermeasures using high-strength steel materials.

Consumer information crash tests, such as the NHTSA's New Car Assessment Program's (NCAP's) full overlap frontal impact and the Insurance Institute for Highway Safety's (IIHS's) small and moderate overlap frontal impacts, have contributed to advance vehicle safety and reduce injury risk in the past. Recent studies have indicated that oblique crashes represent common real-world accident patterns related to belted occupant fatalities [Bean, 2009]. When comparing the number of injuries by body region for oblique and co-linear frontal impacts, it was observed that drivers in left oblique impacts experienced more Maximum Abbreviated Injury Scale (MAIS) 3+ injuries in almost every body region than drivers in co-linear crashes [DOT/NHTSA 2015].

The Center for Collision Safety and Analysis (CCSA) at George Mason University (GMU) has analyzed sixteen left oblique tests conducted by NHTSA regarding intrusion patterns and related injury risk [Zhang, 2015]. Furthermore, 65 oblique and 265 NCAP full overlap tests were analyzed regarding vehicle pulse, intrusion, and injury metrics. While there was no clear trend linking higher intrusion to higher tibia loads, it was found that occupant compartment intrusion, pulse severity, and local effects could contribute to lower extremity injuries. It can be concluded that risk of injury can increase as the maximum intrusion from the occupant compartment increases.

IIHS compared the performance of 25 vehicles in NHTSA's frontal oblique condition and the IIHS small overlap configuration. The selected cars represented a wide range of vehicle sizes. With respect to lower extremity injuries, it was found that 36% (9 cars) of the vehicles exceeded preliminary Injury Assessment Reference Values (IARVs) in the oblique impact, while only 8% (2 cars) exceeded the IARVs for the small overlap configuration [Mueller, 2015]. Differences in vehicle pulse and occupant compartment intrusion were considered to be possible reasons.

The oblique impact test captures the deformations of a significant number of real-world accidents that occur today, and the development of additional countermeasures for restraints and vehicle structure may have the potential to further improve vehicle safety and reduce injury risk in the future. Consequently, NHTSA is considering adopting a frontal oblique impact configuration into its NCAP rating protocol [DOT/NHTSA, 2015].

The developed laboratory test procedure is conducted in combination with a more biofidelic dummy, the Test device for Human Occupant Restraints (THOR) [DOT/NHTSA, 2015]. An Oblique Moving Deformable Barrier (OMDB) was developed to produce target vehicle crush patterns similar to real-world cases [Saunders, 2011]. It has a weight of 2,500 kilograms (kg) and impacts a stationary vehicle at a speed of 90 kilometers per hour (km/h). The vehicle is placed at a 15-degree angle and a 35-percent overlap occurs between the OMDB and the front end of the struck vehicle, as shown in Figure 1.

Figure 1 - Frontal Oblique Test Configuration

Crash test results have shown that vehicles may require structural modifications for good performance in NHTSA's frontal oblique test procedure. In a previous project, that was funded by NHTSA, the GMU Team determined incremental vehicle structural change requirements using steel materials and their associated mass to significantly reduce occupant compartment intrusion.

An available FE model of a mid-size sedan was updated and validated using data from a 2015 Toyota Camry. The generated baseline model correlated well with the New Car Assessment Program (NCAP) full overlap test, NHTSA's left and right oblique impact tests, and with the IIHS small and moderate overlap crash configurations. An iterative process was used to develop countermeasures to significantly reduce occupant compartment intrusion for the left and right oblique impact configuration. No unintended consequences, i.e. no considerable increase of vehicle pulse for oblique and co-linear load cases were observed. The associated added mass was +17 kg using high-strength steel materials.

The aforementioned developed FE model and tools were used to determine if similar results (i.e. similar reduction in occupant compartment intrusion, and no unintended

consequences, such as significantly more severe vehicle pulses) could be achieved using composite materials for select components.

(BLANK)

2. Objective

The objective of this research was to demonstrate necessary changes to a passenger vehicle's structure to significantly reduce occupant compartment intrusion by 60 percent or greater in NHTSA's oblique frontal crash test condition. Structural countermeasures of both the driver's and passenger's sides of the vehicle for left- and right-side oblique impacts were to be developed.

The studied vehicle had to meet the structural intrusion requirements for a “GOOD” or “ACCEPTABLE” structural rating in the IIHS small overlap, “GOOD” rating in the IIHS moderate overlap, and 5-Star rating in the NCAP full frontal test.

In the IIHS moderate overlap configuration, the tested vehicle travels at a speed of 64 km/h with a 40 percent overlap co-linear into a fixed deformable barrier. The vehicle is equipped with a 50th percentile male Hybrid III dummy in the driver seat. The initial structural rating is based on comparison of intrusion measurements with rating guidelines for the upper and lower occupant compartment. For example, intrusions of 15 centimeters or less at the driver’s toe-pan would be rated “GOOD”.

In the IIHS small overlap configuration, the tested vehicle travels at a speed of 64 km/h with a 25 percent overlap co-linear into a fixed rigid barrier. The vehicle is equipped with a 50th percentile male Hybrid III dummy in the driver seat. The initial structural rating is based on comparison of intrusion measurements with rating guidelines for the upper and lower occupant compartment.

In the NCAP full frontal configuration, the tested vehicle travels at a speed of 56 km/h with full overlap co-linear into a rigid wall. The vehicle is equipped with a 50^{th} percentile male Hybrid III dummy in the driver seat and with a 5^{th} percentile female Hybrid III dummy in the passenger seat. The current NCAP rating is based on injury risk assessment rather than occupant compartment intrusion.

A finite element model for an appropriate passenger vehicle that fulfills the above requirements was selected and validated to match the acceleration and intrusion measurements in NCAP frontal full overlap, IIHS moderate and small overlap test procedures. The simulation results were compared to available crash test results using an objective rating methodology. Similarly, baseline simulations for oblique frontal test configurations were conducted and compared to respective test data.

The simulation results were used to establish design goals to minimize occupant compartment intrusion in left- and right-side oblique frontal crashes. Structural countermeasures were developed according to the previously defined design goals. The associated incremental differences in vehicle mass, material, and manufacturing cost between the baseline model and the model with implemented countermeasures were determined.

The effects of implemented structural design changes were also evaluated with respect to vehicle pulse and intrusion characteristics in existing co-linear impact configurations.

(BLANK)

3. Methods

3.1. Vehicle Selection

The vehicle selected for this study was the baseline selected for the NHTSA study using the high strength steels for improving the crash performance in the frontal oblique offset test. Several criteria were used to determine an appropriate vehicle on which to conduct this research. This included evaluation of the number of vehicle sales as a measure of how well it represents mid-size sedans in the United States (US), performance in existing consumer information tests, and availability of an adequate FE simulation baseline model. The vehicle also was required to meet the structural intrusion requirements for a “GOOD” or “ACCEPTABLE” structural rating in the IIHS small overlap crash test, “GOOD” rating in the IIHS moderate overlap crash test, and a 5-Star rating in the NCAP full frontal crash test.

Satisfying the aforementioned criteria, a FE model of a 2012 Toyota Camry, which had been developed by the GMU Team, was used as a starting point. Toyota introduced structural design changes in January 2014. Test results with vehicles that were built after this date are called Model Year (MY) 2015 vehicles in this report.

The NCAP rating is based on occupant injury criteria. The MY 2012 vehicle received five stars for the driver and four stars for the passenger. The MY 2015 vehicle received four stars for the driver and five stars for the passenger. Occupant risk depends on vehicle structure and restraint system performance. Occupant compartment intrusion was small, and the vehicle pulse was judged good for both vehicles. It can be stated that both MYs represent vehicles with structural intrusion characteristics that allow them to receive a Five-Star NCAP rating.

The mid-size sedan received an overall GOOD rating in the 64 km/h IIHS moderate overlap impact with a GOOD sub-rating for the structure and safety cage. This applies to 2012-2016 models. Therefore, the MY 2012 as well as the MY 2015 vehicles meet the structural intrusion requirements for a GOOD rating in the IIHS moderate overlap impact.

Beginning with 2014 models (built after December 2013) the front structure of the mid-size sedan was modified specifically to improve performance in the IIHS 64 km/h small overlap frontal crash test. The MY 2012 received a POOR rating with a POOR sub-rating for structure and safety cage. The MY 2015 received a GOOD overall rating with an ACCEPTABLE sub-rating for structure and safety cage. The MY 2015 meets the structural intrusion requirements for an ACCEPTABLE structural rating in the IIHS small overlap impact.

In addition, left oblique frontal impact tests were conducted by NHTSA with a MY 2012 (test # 9124) and a MY 2015 (test # 8790) vehicle. A right oblique frontal impact test was conducted only for the MY 2012 (# 9121).

In a previous project, a physical vehicle of the mid-size sedan was purchased and a detailed FE model was built using a reverse engineering process. A digitizing device was used to scan all relevant components including their internal structure. Accurate Computer Aided Design (CAD) surfaces were generated and used for FE mesh generation. All components were positioned using a defined reference coordinate system and checked for penetrations. Spot-welds, bead welds, bolts, and joints were used for respective part connections. Material thicknesses and mass distribution were assigned to the individual parts and components. Mass, measured center of gravity (CG) location and inertia properties of the entire vehicle were verified. Material property data for many structural parts was obtained by cutting specimens from the actual vehicle components and conducting material coupon tests.

Most components were modeled using shell elements with an average element size of 6 millimeters (mm). The model was evaluated and validated using the nonlinear, explicit FE code LS-DYNA [Hallquist, 2013] with a minimum time-step of 0.7 microseconds using 16 central processing units on a Hewlett-Packard high-performance computer system. Additional details regarding the modeling approach and validation process can be found in [Reichert, 2016]. The FE model contains relevant structural and interior components, such as body in white, engine, drivetrain, steering, suspension, seats, trims, etc., which are represented by more than 1000 parts and approximately 2.25 million nodes and elements.

Non-destructive analysis of a physical 2015 Toyota Camry and additional information was used to determine differences between the MY 2012 and MY 2015 mid-size sedans. To improve performance in the IIHS small overlap test from POOR to ACCEPTABLE, a spacer was added beyond the bumper reinforcement to the front side member, to direct crash energy through the side member into the reinforced A-pillar, which diffuses it through the roof rail, rocker panel, and floor pan. These changes were phased in as a MY 2014.5 package during December 2013 [SAE, 2016].

Figure 2(a) illustrates the relevant structural differences between MY 2012 and MY 2015. Full-scale crash tests with vehicles that included these changes are called “2015 Toyota Camry” tests in the remainder of this report. Figure 2(b) shows (from right to left) a bottom view of the finite element model with an enlarged view of the added bumper reinforcement extension and “spacer” for the simulation model and the physical vehicle.

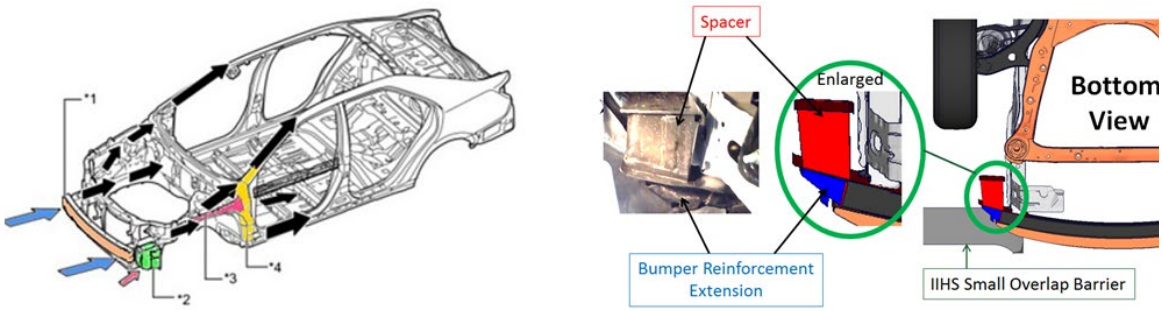

Figure 2 – Design Changes (a) Schematic, (b) "Spacer"

The MY 2012 mid-size sedan FE model was updated accordingly. Full-scale test results showed that the design changes mainly affected performance in the IIHS small overlap impact, while other crash configurations, such as NCAP full overlap and NHTSA left oblique impact, showed similar results for the MY 2012 and MY 2015 vehicles. Advanced modeling techniques for the wheel connection were implemented into the FE model to better represent the failure mechanisms and wheel kinematics seen in the IIHS small overlap impact. The added bumper reinforcement extension and spacer interacts with the IIHS small overlap barrier and activates the frontal rail on the driver side. The deformation of the longitudinal rail contributes to the structural crash energy absorption.

All updates were implemented to the driver and passenger side of the FE model. The associated added vehicle mass was equivalent to 9.7 kg and is like the difference in vehicle mass from NHTSA's left oblique test of a MY 2015 vehicle (test #8790, 1450 kg as delivered, 1734 kg as tested) and a MY 2012 vehicle (test #9124, 1443 kg as delivered, 1759 kg as tested).

Test data from the MY 2015 vehicle was used to evaluate the updated FE model. Even though complete information for all the detailed design changes from MY 2012 to MY 2015 was not available, it was determined that the updated FE model does a good job of simulating the performance of the MY 2015 mid-size sedan in the respective crash configurations. It will be called the "2015 Toyota Camry Baseline Model (BM)" in the remainder of this report.

All baseline simulations were conducted using this model. Developed structural countermeasures to significantly reduce occupant compartment intrusion were evaluated with respect to the BM.

3.2. Baseline Model Validation – Left Oblique Impact

Available full-scale crash test results for NHTSA's left and right oblique impact, NCAP full overlap, IIHS small overlap, and IIHS moderate overlap configurations were used to validate the MY 2015 BM.

In addition, NHTSA's left oblique full-scale impact tests #8790 [Calspan, 2015] and #9124 [Calspan, 2013] were used to evaluate the difference between a MY 2012 and a MY 2015 vehicle in this crash configuration. Both model years showed a similar overall vehicle deformation pattern. Toe-pan intrusion was recorded in both tests. Comparable results, with a maximum intrusion of 94 mm in the MY 2015 and 91 mm in the MY 2012 vehicle, were observed.

Similarly, no significant differences in door-sill deformation were detected. The 2015 vehicle had a maximum value of 39 mm, while the MY 2012 vehicle had a maximum value of 40 mm. With respect to vehicle pulse, again, similar characteristics, with a maximum peak acceleration of 45g for the MY 2012 and 43g for the MY 2015 vehicle, were observed. Hence, NHTSA's left oblique impact full-scale test results for the mid-size sedan showed similar characteristics with respect to vehicle deformation, occupant compartment intrusion, and vehicle pulse.

Overall vehicle deformation and specific occupant compartment intrusion values for the MY 2015 mid-size sedan in test and simulation were compared. Similar deformation of the frontal structure, door frame, and roof were observed. The A-pillar showed minor buckling in both test and simulation. It was noted that there was no significant door sill deformation in either test or simulation. Intrusion along the rocker pillar and minor bending of the A-pillar area were well captured in the simulation model.

Simulations have been run until 200 ms to take spring back effects into account when evaluating intrusions. Accordingly, vehicle pulse comparisons are shown until 200ms. It can be noted that pulse evaluations until 120 ms would be sufficient as well.

Toe-pan intrusion was recorded for measurement points in five rows, consisting of four points each, in test and simulation. In addition, points at the instrument panel, brake pedal and steering wheel were evaluated, as shown in Figure 3.

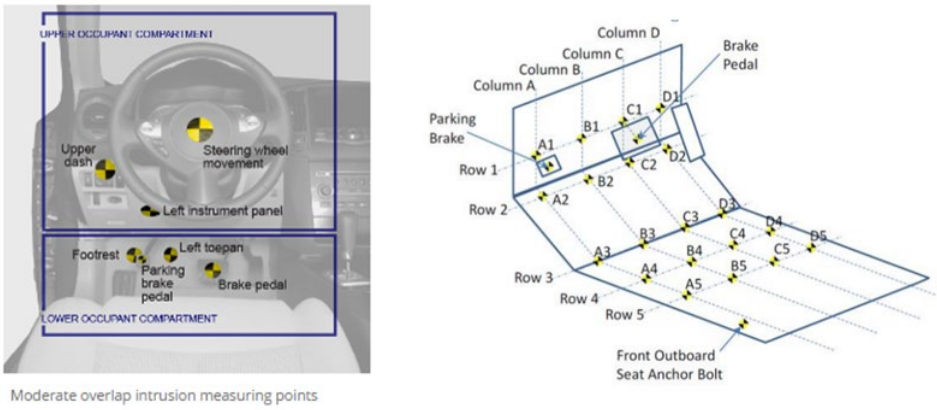

Figure 3 – Intrusion Measurement Points

The highest values occur in row 1, which is the most forward and upward location at the toe-pan. Values decreased for more rearward locations in test and simulation. A maximum intrusion of 94 mm was observed in the test, versus 99 mm in the simulation. Instrument panel intrusion was not significant in either test or simulation. Lower and upper occupant compartment intrusion, including toe-pan deformation from the full-scale crash test, was well captured in the simulation model.

Figure 4 compares x-acceleration pulse for the MY 2015 vehicle in test and BM simulation in the left oblique impact configuration. An accelerometer on the far side rear sill was found to be the most reliable location to evaluate vehicle pulse time history data and was therefore used for the comparison. Test results are depicted using a black solid line and simulation results are depicted using a blue dashed line. Good overall correlation for the acceleration time history data can be observed. Values for maximum peak acceleration (a_{max}), maximum peak acceleration that lasted 5 milliseconds (a_{5ms}), maximum peak acceleration that lasted 15 milliseconds (a_{15ms}) and change in velocity (Δv) correlate well. Time history data was compared using the objective rating tool CORA [Thunert, 2012]. A CORA rating value of 0.94 documents the good correlation between test and simulation.

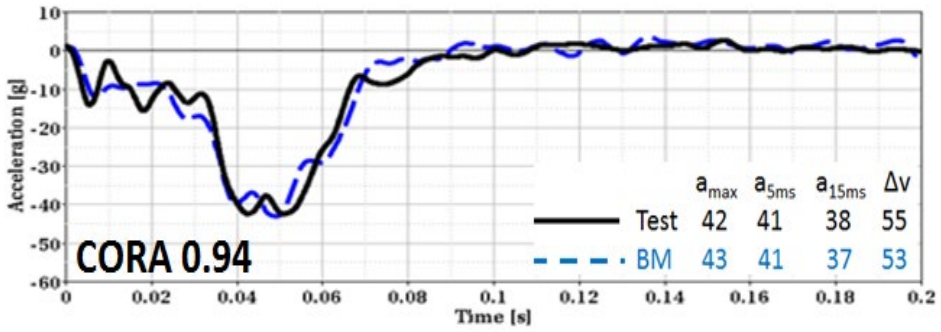

Figure 4 - 2015 Left Oblique Test vs Sim. - Vehicle Pulse

Figure 5 shows the OMDB acceleration pulse time history for the left oblique impact configuration. Test data is depicted as a black solid line and simulation data as a blue dashed line. Good correlation between test and BM simulation can be observed. The objective CORA rating value is 0.95.

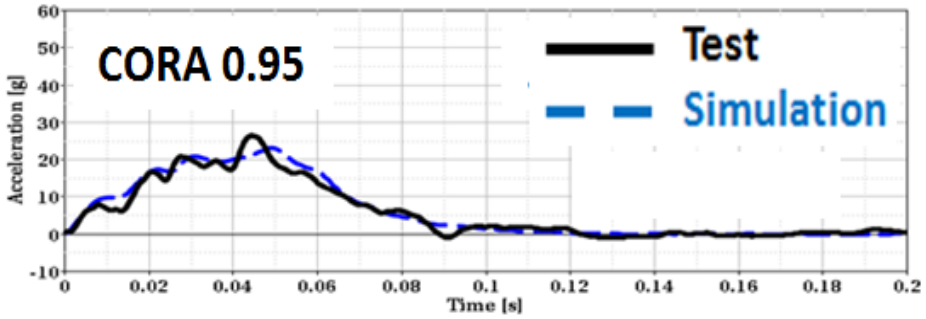

Figure 5 - 2015 Left Oblique Test vs Sim. - Barrier Pulse

Additional information regarding validation results including the comparison of intrusions can be found in “Development of a 2015 Mid-Size Sedan Vehicle Model” [Reichert, 2017].

3.3. Baseline Model Validation – Right Oblique Impact

NHTSA's right oblique impact test #9121 [Calspan, 2013] of the MY 2012 vehicle was used to evaluate the developed BM.

No full-scale test data of the right oblique configuration of the MY 2015 vehicle was available. Hence, an evaluation was undertaken to determine how the vehicle performed in the left oblique impact. Test results for the left oblique impact configuration showed similar vehicle deformation, intrusion, and vehicle pulse characteristics for MY 2012 and MY 2015 mid-size sedan, as previously outlined. Therefore, it was assumed, that the MY 2012 and MY 2015 vehicle also would perform similarly in the right oblique condition. To evaluate results of the MY 2015 FE model, the available data of the full-scale test with the MY 2012 mid-size sedan was used to compare the right oblique baseline simulations.

Similar deformation of the frontal structure, door frame, and roof were observed. The A-pillar showed minor buckling in test and simulation. The maximum door sill deformation values were 38 mm for the test and 35 mm for the simulation. Door sill deformation was considered moderate in test and simulation. Intrusion along the rocker pillar and minor bending of the A-Pillar area were well captured in the simulation model. Toe-pan intrusion was recorded for measurement points in 5 rows, consisting of 3 points each, in test and simulation. The highest values occur in row 1, which is the most forward and upward location at the toe-pan. Values decrease for more rearward locations in both test and simulation. A maximum intrusion of 163 mm in row 1 was observed in the simulation and 131 mm in the test.

Figure 6 compares vehicle x-acceleration pulse in test and BM simulation for the right oblique impact configuration. As before, test results are depicted as a black solid line and simulation results are depicted as a blue dashed line. Good overall correlation can be observed. Values for maximum peak acceleration (a_{max}), maximum peak acceleration that lasts 5 milliseconds (a_{5ms}), maximum peak acceleration that lasts 15 milliseconds (a_{15ms}), and Δv compare well. An objective CORA rating value of 0.93 documents the good correlation between test and simulation.

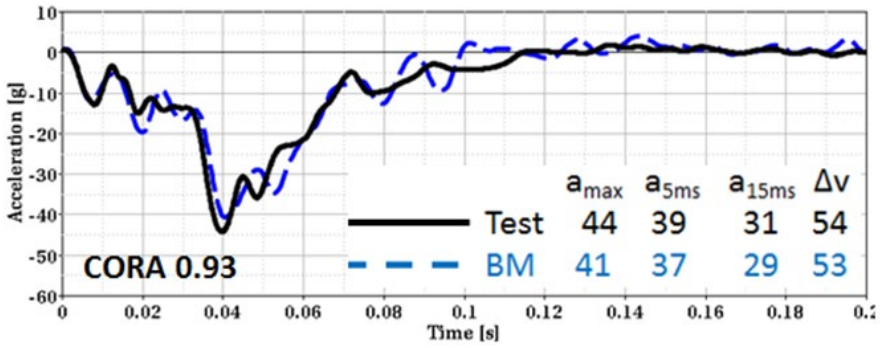

Figure 6 - Right Oblique Test vs Sim. - Vehicle Pulse

Figure 7 shows the OMDB barrier acceleration pulse for the right oblique impact configuration. Here again, test data is depicted by a black solid line and simulation data by a blue dashed line. Good correlation between test and BM simulation can be observed. The CORA rating value is 0.95.

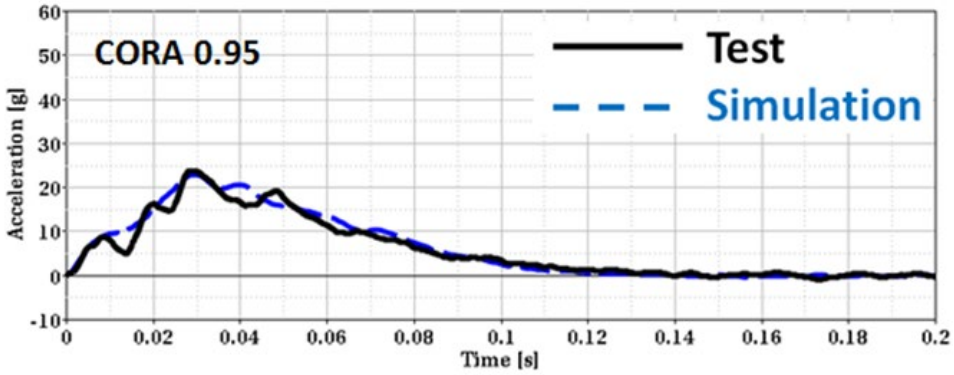

Figure 7 - Right Oblique Test vs Sim. - Barrier Pulse

Assuming similar pulse characteristics for the MY 2015 and MY 2012 vehicle for the right oblique configuration, as seen for the left oblique impact, the BM represents well the vehicle and barrier pulse characteristics of a MY 2015 mid-size sedan in the right oblique impact configuration.

3.4. Baseline Model Validation – Co-Linear Impacts

The baseline model was also validated against full-scale crash test results for NHTSA's full frontal NCAP, as well as IIHS small and moderate overlap impacts.

IIHS Small Overlap (SO) test CEN1349 [IIHS, 2015] of the MY 2015 mid-size sedan traveling at 64 km/h into a fixed rigid barrier with a 25% overlap was used to evaluate the developed simulation BM. Figure 8 shows the overall vehicle deformation in the baseline simulation and in the full-scale crash test. Similar deformation of the frontal structure, door frame, and roof were observed. The A-pillar showed noticeable buckling in both test and simulation. The failure mechanism of the wheel to control-arm connection and overall wheel kinematics were well captured.

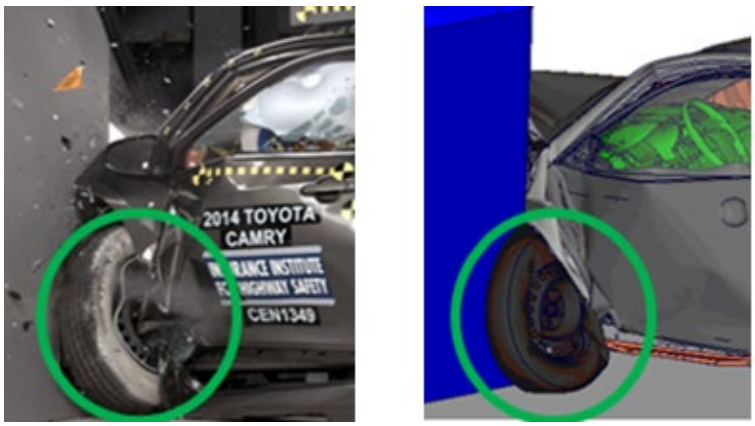

Figure 8 – IIHS Small Overlap – Test vs. Simulation

Intrusion for the lower and upper occupant compartment according to the IIHS SO rating protocol is shown in Figure 9. The test results are shown using black solid line and BM simulation results are shown using a blue line. Test and simulation results correlated well, resulting in an ACCEPTABLE structural rating for both test and BM simulation. It can be stated that the BM captures the overall and door sill deformation seen in the full-scale crash test reasonably well. Occupant compartment intrusion characteristics were well captured in the simulation. Additional information for IIHS small and moderate overlap and NCAP full overlap correlation can be found in [IIHS, 2013].

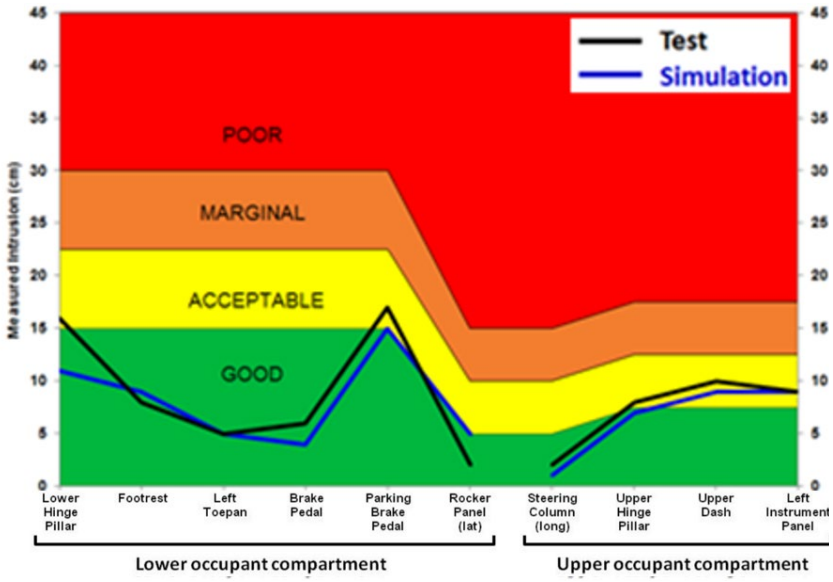

Figure 9 – IIHS Small Overlap Test vs Sim. – Intrusion

The updated FE model well represented the structural performance of a MY 2015 mid-size sedan in existing crash configurations, as well as in NHTSA's left and right oblique impact tests. Therefore, it was used as the reference model to develop structural countermeasures for significantly reducing occupant compartment intrusion for left and right oblique crash configurations. The developed model with respective structural countermeasures made out of high strength steel will be called "Countermeasure Model Steel" (CM Steel). The developed model with respective structural countermeasures made out of composite material will be called "Countermeasure Model Composite" (CM Composite). In addition to comparing BM and CM in left and right oblique impact conditions, it also was used to analyze how introduced countermeasures affected vehicle crash characteristics in existing co-linear impact configurations, i.e. IIHS SO, MO and NCAP full overlap.

3.5 Design Goals and Mass Analysis

The results of the BM simulations and available full-scale crash tests were used to determine design goals to significantly reduce occupant compartment intrusion in NHTSA's left and right oblique impact condition. The performance target was significant reduction of maximum absolute occupant compartment intrusion while maintaining moderate vehicle crash pulses.

Significant occupant compartment intrusion was observed in the toe-pan area for the left and right oblique crash conditions. Therefore, the main design goal was to reduce maximum occupant compartment intrusion by at least 60%.

Structural countermeasures can influence the vehicle acceleration pulse and consequently occupant injury risk and restraint system performance. A significant increase in vehicle pulse would be considered an unintended consequence and was monitored. Observed vehicle pulses in full-scale crash tests and baseline simulations were considered moderate.

An iterative process was used to achieve the design goal set. When developing countermeasures, the aim was to make as few modifications to the overall vehicle structure and to allow a genuine mass analysis. Re-designing the front structure of the vehicle for the oblique impact condition, which might lead to better mass production and cost saving, was beyond the scope of this project.

Using the baseline model (BM), which represents a 2015 Toyota Camry, as a reference, structural countermeasures using high-strength steel, as well as composite materials, were developed. Added and modified components were evaluated with respect to incremental change in mass. The overall associated incremental difference in vehicle mass between the BM and the CM was determined.

3.6. CFRP Composite Material Validation

In a previous study [Park 2012], a braided carbon-fiber thermoset composite material was selected as the steel substitute in the vehicle structures. Many material tests and numerical simulations were conducted to identify its material characteristics for a Carbon Fiber Reinforced Plastic (CFRP). Their results are described in the project report [Park 2012]. A brief summary of these is described in this section. The developed and validated material card was used for select components when developing structural countermeasures to reduce occupant compartment intrusion in NHTSA's oblique impact configuration.

Tri-axial braided composites can offer an isotropic design by using axial and angled fiber bundles in a single plan. Braided composites also offer better damage resistance, torsional stability, and bending strength compared to unidirectional or weaved composites. Tri-axial braided composites have been used in the commercial aerospace and automotive industry for over 20 years. They are well suited for components that are of simple geometry and need to provide off-axis as well as unidirectional strength. In addition, various studies using braided composites have been conducted and published.

The selected braided CFRP composite used for the material tests is described as follows. The carbon fiber was Torayca T700S C 12000, manufactured by Toray Carbon Fibers America, Inc. The braid architecture is 0°/±60° 2D triaxial (2D3A), as shown in Figure 10. The axial fiber tows contained 24K fibers. The bias tows contained 12K fibers. The resin was Epon 862 epoxy with an Epikure W curing agent, both manufactured by Momentive.

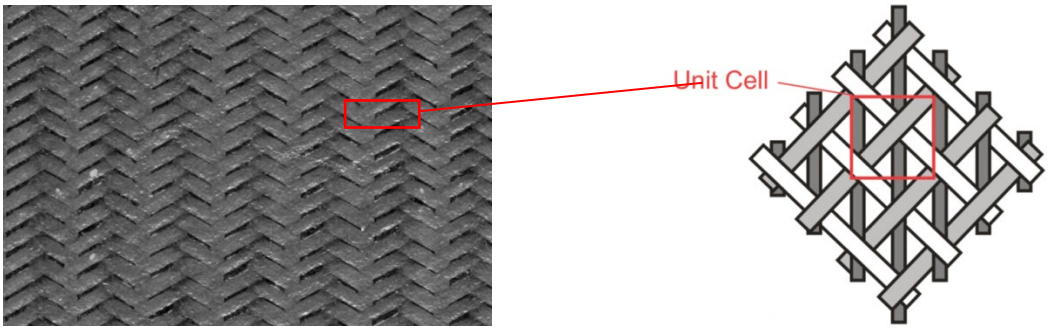

(a) (b)

Figure 10 - 2D3A braided composite: (a) panel, (b) unit cell.

Tension, compression and shear coupon tests were performed in two different directions (axial and transverse) and at four different loading rates. The tension test used two different types of specimens; a standard specimen and a bowtie specimen. A total of 72 coupon tests were conducted. Tube compression tests were performed with three different loading rates. A total of 17 tube tests were conducted. Their test specimens are shown in Figure 11, and their test data are summarized in Table 1 and Table 2.

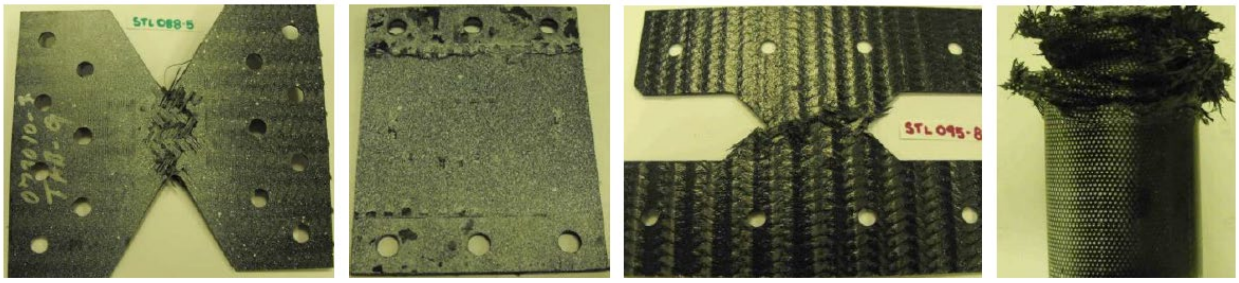

(a) (b) (c) (d)

Figure 11 - Specimens: (a) tension, (b) compression, (c) shear, (d) tube compression.

Table 1 - Data summary for coupon tests

test	direction	rate (m/min)	engineering breaking stress [MPa]	normalized peak stress to 56 vol % fiber [MPa]	engineering breaking strain [%]	elastic modulus [GPa]	Poisson's ratio
ASTM D3039 tension	axial	0.00127	857		1.95	43.3	0.31
	transverse		337		1.44	34.7	0.32
bowtie tension	axial	0.00127	798	775	1.31	67.0	0.25
		0.5	865	815	1.44	66.4	0.36
		5	803	782	1.27	80.6	0.38
		50	783	744	1.33	85.4	0.40
		avg.	812	779	1.34	74.9	
	transverse	0.00127	965	942	2.07	66.4	0.01 - 0.36
		0.5	1017	992	1.72	116.0	0.25 - 0.60
		5	1046	1026	2.02	81.9	0.03 - 0.47
		50	918	950	2.34	57.9	0.03 - 0.06
		avg.	987	978	2.04	80.6	
compression	axial	0.00127	283	282	0.64	51.7	
		0.05	252	237	0.73	34.5	
		0.5	284	271	0.71	40.7	
		5	280	269	0.76	37.7	
		avg.	275	265	0.71	41.2	
	transverse	0.00127	226	221			
		0.05	265	249	0.72	39.3	
		0.5	288	271	0.75	40.1	
		5	305	288	0.74	45.0	
		avg.	271	257	0.74	41.5	
shear	axial	0.00127	180	177	0.75	32.9	
		0.5	190	188	0.83	28.5	
		5	177	174	0.72	25.5	
		50	201	199	0.84	26.0	
		avg.	187	185	0.79	28.2	
	transverse	0.00127	200	195	0.75	29.2	
		0.5	218	212	0.86	28.5	
		5	239	233	0.86	32.9	
		50	226	216	0.86	33.4	
		avg.	221	214	0.83	31.0	

Numerical simulations of the material tests and tube compression tests were conducted to develop the numerical material model of the CFRP composite. The MAT58 in the material database of LS-DYNA was utilized for the braided composite. The

material properties of MAT58 for the braided composite can be obtained directly from coupon test results listed in Table 1.

Table 2 - Data summary of tube compression tests

		Median Crush Load* [kN]	Median Crush Stress* [MPa]	Median Stress Normalized to 56% Fiber Volume [MPa]	Specific Sustained Crushing Stress [SSCS] [MPa]	Crush Compression Ratio**	Specific Energy Absorption(1) with folding mode failure [SEA-FM] [kJ/kg]	Specific Energy Absorption(2) [SEA] [kJ/kg]	Specific Energy Absorption(3) [SEA] [kJ/kg^2]	Range of Peak Temperatures During Crush [°C]
1.5 m/min 0.0254 m/s	Average	47.0	74.9	95.8	51.5	0.35	43.3	53.3	19.9	-
	Std.Dev.	3.66	5.79	9.61	4.29	0.04	2.96	4.56	2.00	-
	Coeff. of Var. [%]	7.78	7.74	10.0	8.32	10.0	6.84	8.56	10.0	-
140 m/min 2.4 m/s	Average	47.8	77.1	97.4	53.2	0.36	-	52.5	20.9	173-362
	Std.Dev.	2.14	3.44	4.55	2.01	0.02	-	2.30	0.81	
	Coeff. of Var. [%]	4.48	4.46	4.67	3.77	4.67	-	4.37	3.89	
440 m/min 7.4 m/s	Average	43.3	69.2	85.8	47.8	0.32	-	48.9	19.0	254-308
	Std.Dev.	2.35	3.24	3.77	1.95	0.01	-	1.95	0.94	
	Coeff. of Var. [%]	5.43	4.69	4.39	4.08	4.39	-	3.98	4.96	

1) SEA calculated using E_s= Work/(area*density*[actuator displacment + displacement of folded length])

2) SEA calculated using E_s= Work/(area*density*total actuator displacement)

3) SEA for design purposes E_s=Work(displacement at peak - displacement at end)/(mass of tube*displacment at end)

The peak temperatures exceeded the calibration curve maximum of 200°C for all but one of the specimens.

Table 3 shows the values of the material variables of MAT58. Mostly, average values from the coupon tests were taken for determining the moduli, failure stresses, failure strains, and Poisson's ratio. The values of the post-failure parameters of MAT58 (slimit1, slimit2, slimic1, slimic2, and slims) listed in Table 3 were chosen based on the Force-Deflection curves [Park 2012]. The material properties were verified and validated by conducting coupon test simulations and tube compression test simulations.

Table 3 - Material properties of MAT58

Card1	MID	RO	EA	EB		PRBA	TAU1	GAMMA1
		1.5e-9	80000	80000		0.35	0.0	0.0
Card2	GAB	GBC	GCA	SLIMT1	SLIMC1	SLIMT2	SLIMC2	SLIMS
	30000	30000	30000	0.3	1.0	0.1	1.0	0.4
Card3	AOPT	TSIZE	ERODS	SOFT	FS			
			0.5		1.0			
Card4	XP	YP	ZP	A1	A2	A3		
Card5	V1	V2	V3	D1	D2	D3	BETA	
Card6	E11C	E11T	E22C	E22T	GMS			
	0.01	0.015	0.01	0.02	0.01			
Card7	XC	XT	YC	YT	SC			
	300	850	300	1000	200			

(BLANK)

4. Results and Discussion

4.1. Crash Mechanism Analysis

The development of structural countermeasures to significantly reduce occupant compartment intrusion in NHTSA's oblique impact condition requires a thorough understanding of crash mechanisms. The conducted baseline simulations were analyzed with respect to crash mechanisms that specifically contribute to the observed intrusion in left and right oblique impacts.

Local buckling of the firewall was found to be a major factor. Highest intrusion values were observed for toe-pan measurement points in row 1, which represent the most forward and upward locations. It was found that the load transferred through the longitudinal rail contributed to the maximum intrusion values. It can be noted that the load introduced through the frontal rails is being leveraged through the difference in height between the frontal rail and the bottom of the mid-rails. The load introduced through the frontal rail contributes to the maximum intrusion values and local buckling of the toe-pan.

Local buckling of the mid-rails also contributed to the observed occupant compartment intrusion. It was found that there was a significant amount of deformation occurring in the right mid-rail. The parking brake on the driver side is connected to the rocker pillar and the toe-pan area. It acts as a reinforcement of the rocker pillar area on the driver side. Since there is no equivalent component on the passenger side, a significant amount of deformation of the right rocker pillar components was observed in the right oblique impact configuration. Deformation of the rocker pillar components on the passenger side contributed to the maximum occupant compartment intrusion in the right oblique impact.

A firewall support component around the steering column exists on the driver side. The absence of an equivalent firewall support component on the passenger side contributed to the maximum occupant compartment intrusion in the right oblique impact.

4.2. Development of Structural Countermeasures

Three sets of countermeasures using high-strength steel materials were developed to meet the defined design goals in the previous project, funded by NHTSA. The countermeasure model (“CM-Steel”) that showed the highest amount of occupant compartment intrusion reduction is discussed in this report. It serves as reference for the countermeasure model using composite material (“CM-Composite”). Occupant compartment intrusion was reduced by more than 60% compared to the baseline model (BM).

Figure 12 presents an overview of the implemented modifications for CM-Steel.

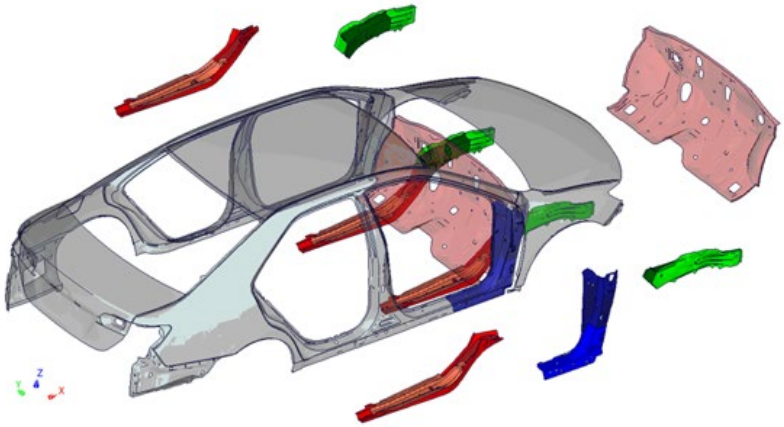

Figure 12 – CM Steel - Structural Countermeasures

The firewall, three components of the right hinge pillar, two parts of the left and right frontal rails, and three parts of the left and right mid-rails were modified.

In order to reduce maximum toe-pan intrusion and local buckling, material thickness and material strength were increased for the firewall, shown in pink. Material thickness was also increased for three components of the right hinge pillar, shown in blue. For the inner hinge pillar (a) and the middle hinge pillar (b) material strength was also increased. The material strength for the outer hinge pillar (c) was not changed in order to allow the same manufacturing stamping process used for the BM. Changes to the right hinge pillar contributed to reduced intrusion and reduced local buckling, specifically in the right oblique impact. The parking brake on the driver side acts as a reinforcement of the hinge pillar area on the driver side. Therefore, the left hinge pillar components were not changed.

In order to reduce the load induced into the firewall, material thickness for two parts of the left and right frontal rails, shown in green, were marginally reduced. This contributed to reduction in maximum toe-pan intrusion and local buckling.

An evaluation was undertaken to determine if a similar reduction of occupant compartment intrusion can be achieved by using composite for the firewall component. Three different thicknesses, i.e. 1.2 mm (2 layers), 2.4 mm (4 layers), and 3.6 mm (6 layers) were evaluated. The associated change in vehicle mass for the CM-Composite vehicles compared to the BM was -15kg, -11kg, and -7kg, respectively.

4.3. Results - Left Oblique Impact

CM-Steel simulation results were compared against the respective BM simulation in NHTSA's left oblique impact configuration. The maximum toe-pan intrusion was reduced by more than 60%. Figure 13 shows a cross-section view of the left passenger compartment. The black line represents the un-deformed "pre-crash" vehicle. The red line represents the deformed shape of the baseline model with high occupant compartment intrusion. The green line shows the deformed shape of the CM-Steel vehicle with a significant reduction of intrusion compared to the BM. The associated change in mass when using countermeasures made out of steel, was +17 kg compared to the BM. Detailed mass and cost analysis for the CM-Steel vehicle can be found in Appendix A1.

The dark red line represents the CM-Composite 1 vehicle, where a composite material made out of two layers was used for the firewall. Intrusion was as high as for the BM and the associated change in mass was -15 kg. The yellow line shows the CM-Composite 2 vehicle with 4 layers of composite and an associated change in mass of -11 kg. Intrusion was reduced compared to the BM but was still significantly higher than for the CM-Steel vehicle. The blue line represents the CM-Composite 3 vehicle with 6 layers of composite. The respective thickness was 3.6 mm and the associated reduction in mass compared to the BM was -7kg. Similar reduction of occupant compartment intrusion was achieved with the CM-Composite 3 model compared to the CM-Steel vehicle. However, instead of adding 17 kg to the total vehicle mass when using steel countermeasures, a reduction of 7 kg was achieved when using composite countermeasures. The CM-Composite 3 vehicle will also be called "CM-Composite" in the remainder of this report.

.

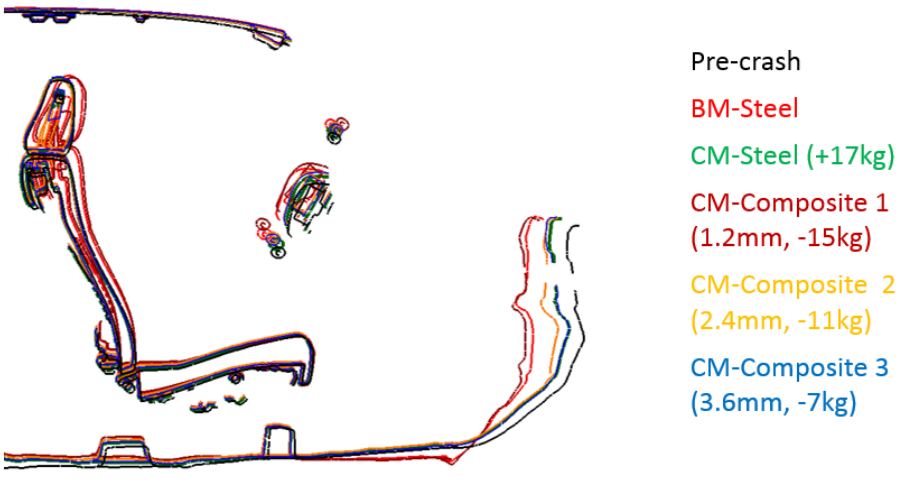

Figure 13 – Left Oblique Intrusion- Baseline vs. CM-Steel and CM-Composite

Material failure was considered in the conducted analysis. No significant failure was observed in the CM-Composite 3 vehicle with a 3.6 mm firewall. Material failure was

observed for the CM-Composite 1 vehicle, as shown in Figure 14. The deformed shape of firewall in the BM, CM-Steel, and CM-Composite 1-3 vehicle in NHTSA's left oblique impact can be found in Appendix A2.

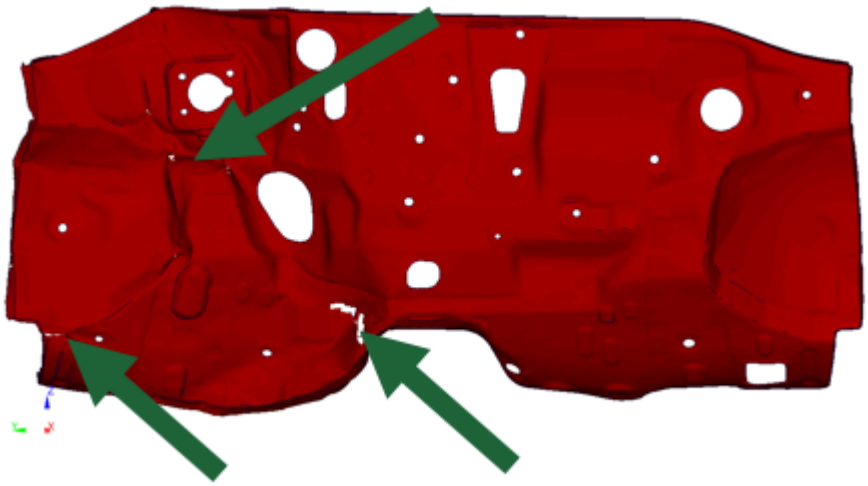

Figure 14 – Left Oblique – Local Material Failure for CM-Composite 1

Figure 15 shows the vehicle pulse, measured at the rear of the vehicle and processed using a SAE 60 filter. An overall similar vehicle pulse was observed for the CM-Steel vehicle, shown in green, and the CM-Composite vehicle, shown in blue. The maximum peak of both vehicles was only marginally higher than measured for the BM, shown in red. The vehicle pulses in the BM, CM-Steel, and CM-Composite 1-3 vehicles in NHTSA's left oblique impact can be found in Appendix A3.

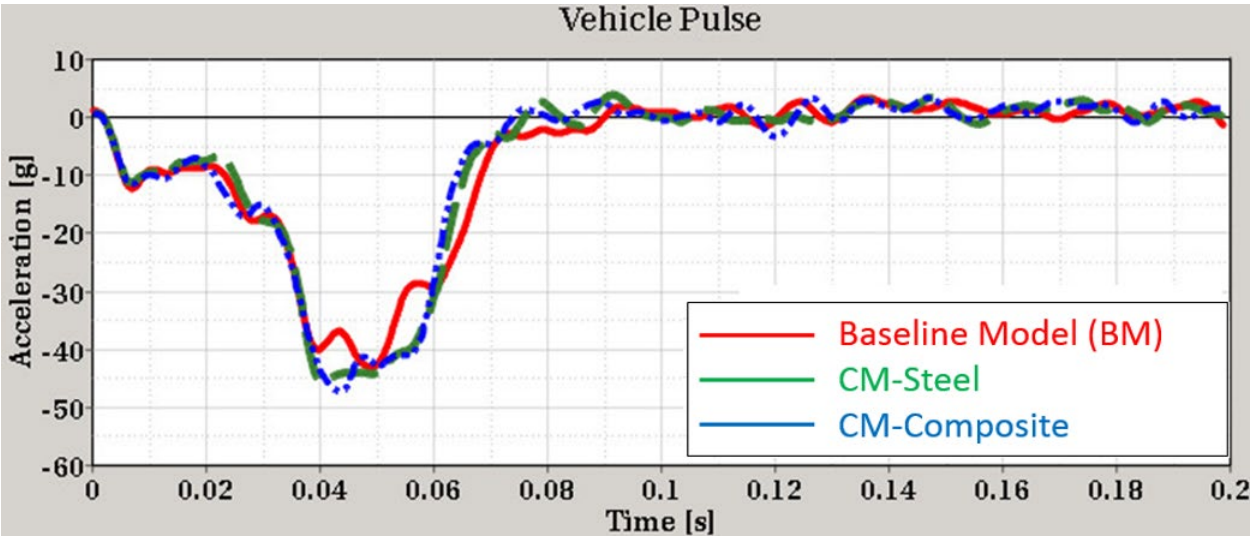

Figure 15 – Left Oblique Vehicle Pulse - BM vs. CM-Steel and CM-Composite

No significant effect with respect to restraint system performance and occupant injury risk due to the introduced structural changes for CM-Steel and CM-Composite was therefore predicted.

4.4. Results - Right Oblique Impact

CM-Steel simulation results were compared against the respective BM simulation in NHTSA's right oblique impact configuration. The maximum toe-pan intrusion was reduced by more than 60% reduction. Figure 16 shows a cross-section view of the left passenger compartment. The black line represents the un-deformed "pre-crash" vehicle. The red line represents the deformed shape of the baseline model with high occupant compartment intrusion. The green line shows the deformed shape of the CM-Steel vehicle with a significant reduction of intrusion compared to the BM. The associated change in mass when using countermeasures made out of steel, was +17 kg compared to the BM. The dark red line represents the CM-Composite 1 vehicle, where 2 layers of composite material were used for the firewall. Intrusion was as high as for the BM and the associated change in mass was -15 kg. The yellow line shows the CM-Composite 2 vehicle with 4 layers of composite and an associated change in mass of -11 kg. Intrusion was reduced compared to the BM but was still significantly higher than for the CM-Steel vehicle. The blue line represents the CM-Composite 3 vehicle with 3 layers of composite. The respective thickness was 3.6 mm and the associated reduction in mass compared to the BM was -7kg. Similar reduction of occupant compartment intrusion was achieved with the CM-Composite 3 model compared to the CM-Steel vehicle. However, instead of adding 17 kg to the total vehicle mass when using steel countermeasures, a reduction of 7 kg was achieved when using composite countermeasures.

.

Figure 16 – Right Oblique Intrusion- Baseline vs. CM-Steel and CM-Composite

Material failure was considered in the conducted analysis. No significant failure was observed in the CM-Composite 3 vehicle with a 3.6 mm firewall. Material failure was observed for the CM-Composite 1 vehicle, as shown in Figure 17. The deformed shape of firewall in the BM, CM-Steel, and CM-Composite 1-3 vehicle in NHTSA's right oblique impact can be found in Appendix A4.

Figure 17 – Right Oblique – Local Material Failure for CM-Composite 1

Figure 18 shows the vehicle pulse, measured at the rear of the vehicle and processed using a SAE 60 filter. An overall similar vehicle pulse was observed for the CM-Steel vehicle, shown in green, and the CM-Composite vehicle, shown in blue. The maximum peak of both vehicles was only marginally higher than measured for the BM, shown in red. The vehicle pulses in the BM, CM-Steel, and CM-Composite 1-3 vehicles in NHTSA's left oblique impact can be found in Appendix A5.

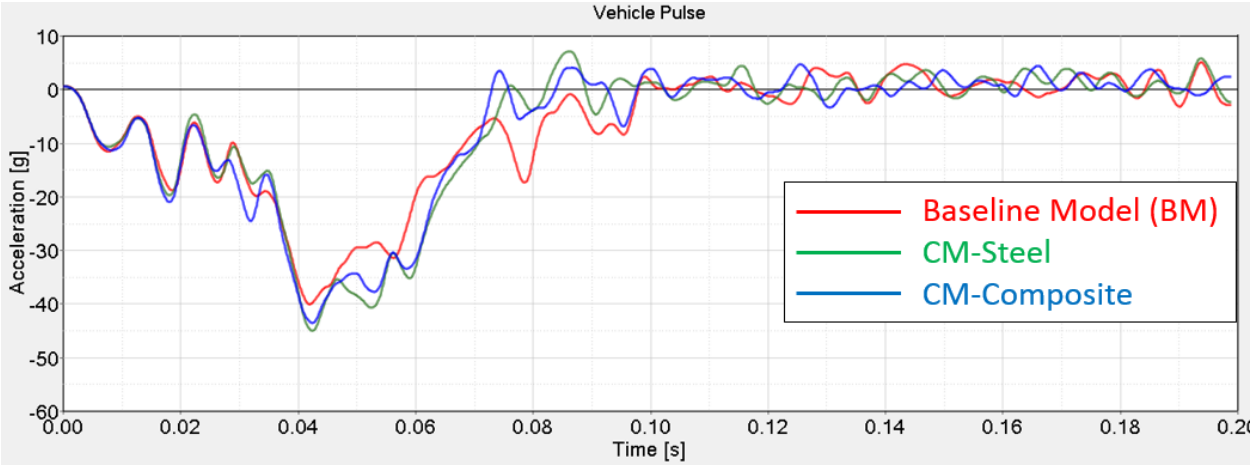

Figure 18 – Right Oblique Vehicle Pulse - BM vs. CM-Steel and CM-Composite

No significant effect with respect to restraint system performance and occupant injury risk due to the introduced structural changes for CM-Steel and CM-Composite was therefore predicted.

4.5. Results – NCAP Full Overlap

In the NCAP full frontal configuration, the tested vehicle travels at a speed of 56 km/h with full overlap co-linear into a rigid wall. In the full-scale test, the vehicle is equipped with a 50th percentile male Hybrid III dummy in the driver seat and with a 5th percentile female Hybrid III dummy in the passenger seat. The current NCAP rating is based on injury risk assessment rather than occupant compartment intrusion.

The effect of structural countermeasures developed for NHTSA's oblique impact was evaluated for the NCAP full overlap load case. The CM-Steel vehicle with countermeasures using high-strength steel (+17kg) and the CM-Composite vehicle with 6 layers (-7kg) were evaluated with respect to the baseline model.

Figure 19 shows a cross-section view on the driver side. The geometrical shape of the vehicle "pre-crash" is shown in black. The deformed shape of the BM after the vehicle has impacted a rigid wall at 56 km/h is shown in red. The occupant compartment intrusion is smaller than for the oblique impact configurations. The vehicle with countermeasures out of high-strength steel (CM-Steel) is shown in green and the CM-Composite vehicle is depicted in blue. No significant occupant compartment intrusion was observed for either countermeasure models. CM-Steel and CM-Composite resulted in a reduction of occupant compartment intrusion compared to the BM in NHTSA's NCAP full overlap load case.

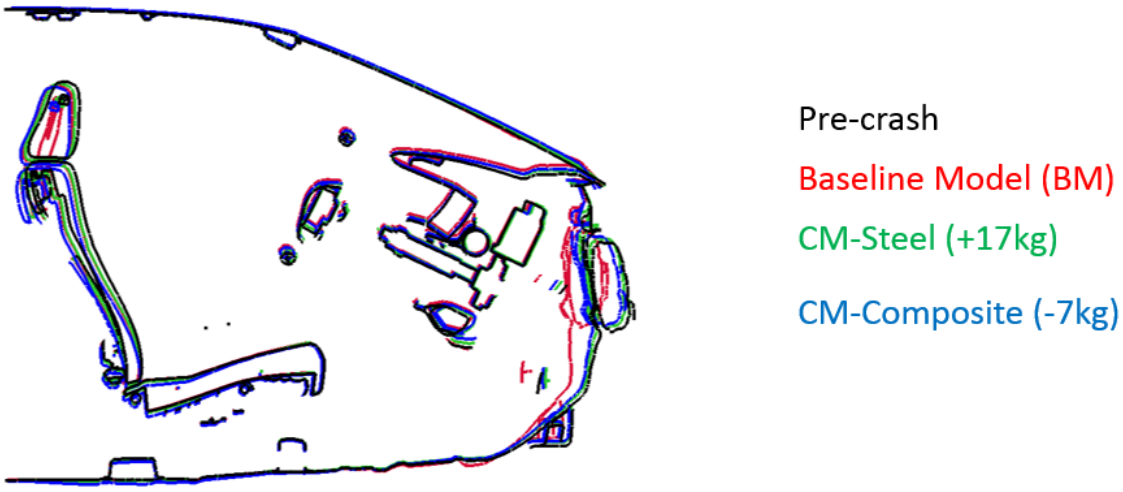

Figure 19 – NCAP Full Overlap – BM vs. CM-Steel and CM-Composite

Figure 20 shows the vehicle pulse, measured at the rear of the vehicle and processed using a SAE 60 filter. An overall similar vehicle pulse was observed for the CM-Steel vehicle, shown in green, and the CM-Composite vehicle, shown in blue. The

maximum peak of both vehicles was similar to the BM, shown in red. While the first peak, caused by initial contact of the rigid barrier with the engine, was the same for the BM and CM-Steel, the initial peak was marginally lower for the CM-Composite vehicle. The second peak at about 50ms showed the opposite trend. The CM-Composite vehicle showed a marginally higher peak compared to the BM and CM-Steel.

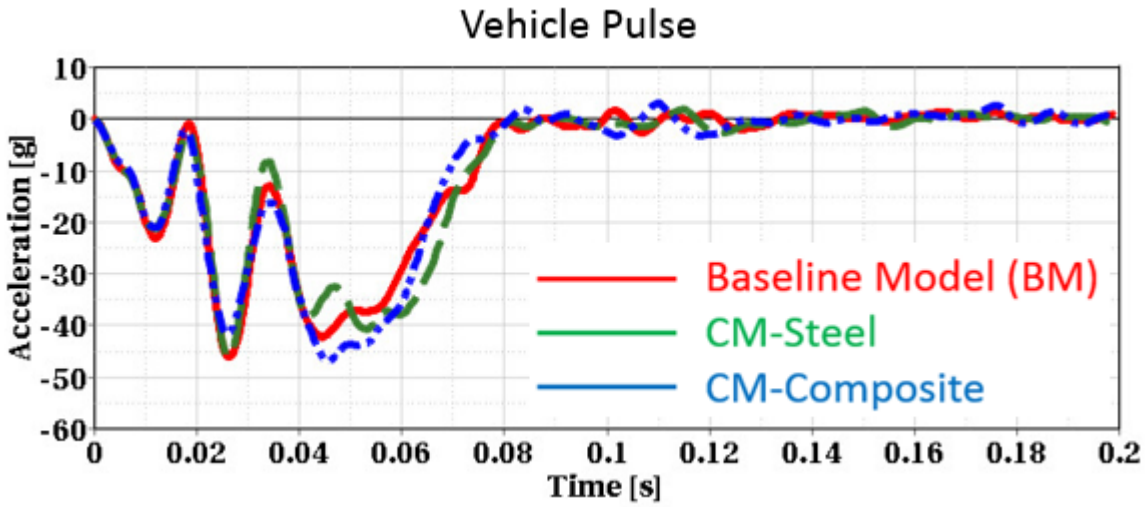

Figure 20 – NCAP Vehicle Pulse – BM vs. CM-Steel and CM-Composite

No significant effect with respect to restraint system performance and occupant injury risk due to the introduced structural changes for CM-Steel and CM-Composite was therefore predicted.

4.6. Results – IIHS Moderate Overlap (40%)

In the IIHS moderate overlap configuration, the tested vehicle travels at a speed of 64 km/h with a 40 percent overlap co-linear into a fixed deformable barrier. In the full-scale test, the vehicle is equipped with a 50th percentile male Hybrid III dummy in the driver seat. The structural rating is based on comparison of intrusion measurements with rating guidelines for the upper and lower occupant compartment.

The effect of structural countermeasures developed for NHTSA's oblique impact was evaluated for the IIHS moderate overlap load case. The CM-Steel vehicle with countermeasures using high-strength steel (+17kg) and the CM-Composite vehicle with six layers (-7kg) were evaluated with respect to the baseline model.

Figure 21 shows a cross-section view on the driver side. The geometrical shape of the vehicle "pre-crash" is shown in black. The deformed shape of the BM after the vehicle impact is shown in red. A significant amount of occupant compartment intrusion can be observed for the BM. The vehicle with countermeasures out of high-strength steel (CM-Steel) is shown in green and the CM-Composite vehicle is depicted in blue. No significant occupant compartment intrusion was observed for either countermeasure models. CM-Steel and CM-Composite resulted in a reduction of occupant compartment intrusion compared to the BM in the IIHS moderate overlap load case.

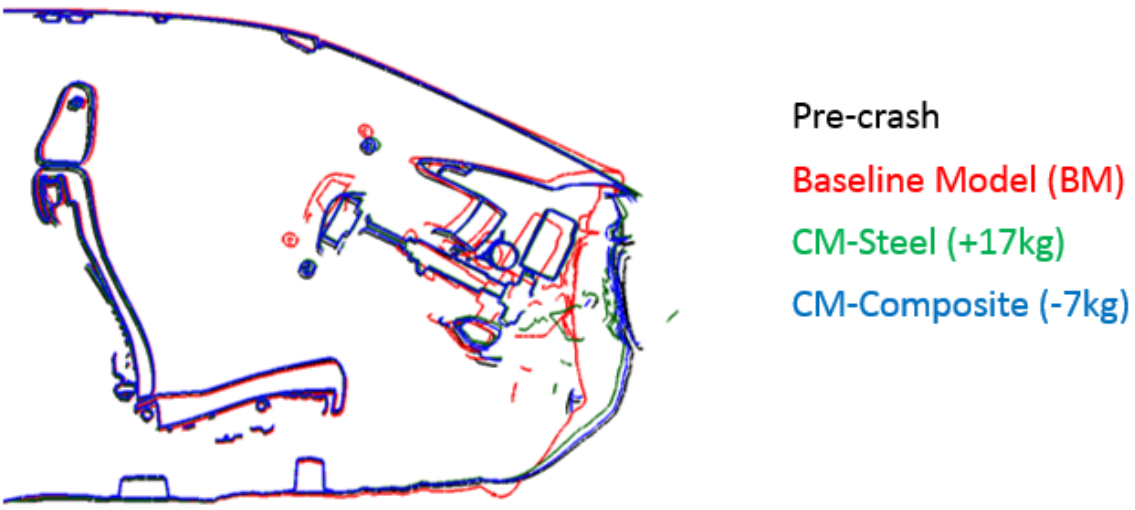

Figure 21 – IIHS Moderate Overlap – BM vs. CM-Steel and CM-Composite

Figure 22 shows the vehicle pulse, measured at the rear of the vehicle. An overall similar vehicle pulse was observed for the CM-Steel vehicle, shown in green, and the CM-Composite vehicle, shown in blue. The maximum peak of both vehicles was similar

to the BM, shown in red. The maximum peak of the CM-Steel vehicle was slightly lower than the BM. The peak of the CM-Composite vehicle occurred marginally earlier than the BM.

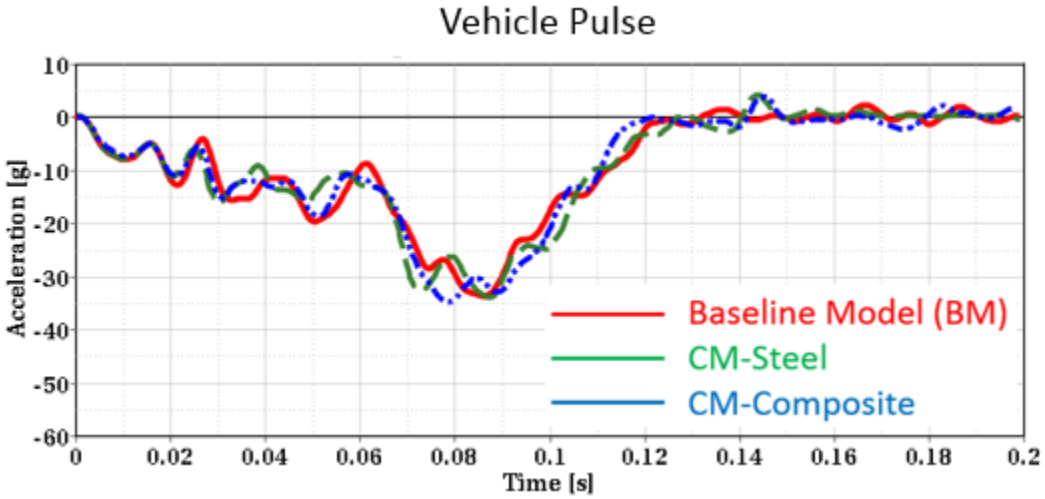

Figure 22 – IIHS MO Vehicle Pulse – BM vs. CM-Steel and CM-Composite

No significant effect with respect to restraint system performance and occupant injury risk due to the introduced structural changes for CM-Steel and CM-Composite was therefore predicted.

4.7. Results – IIHS Small Overlap (25%)

In the IIHS small overlap configuration, the tested vehicle travels at a speed of 64 km/h with a 25 percent overlap co-linear into a fixed rigid barrier. In the full-scale test, the vehicle is equipped with a 50th percentile male Hybrid III dummy in the driver seat.

The effect of structural countermeasures developed for NHTSA's oblique impact was evaluated for the IIHS small overlap load case. The CM-Steel vehicle with countermeasures using high-strength steel (+17kg) and the CM-Composite vehicle with six layers (-7kg) were evaluated with respect to the baseline model.

Figure 23 shows a cross-section view on the driver side in the IIHS small (25%) overlap configuration. The geometrical shape of the vehicle "pre-crash" is shown in black. The deformed shape of the BM after the vehicle impact is shown in red. A similar amount of occupant compartment intrusion can be observed for the BM, the vehicle with countermeasures out of high-strength steel (CM-Steel), shown in green, and the CM-Composite vehicle, depicted in blue.

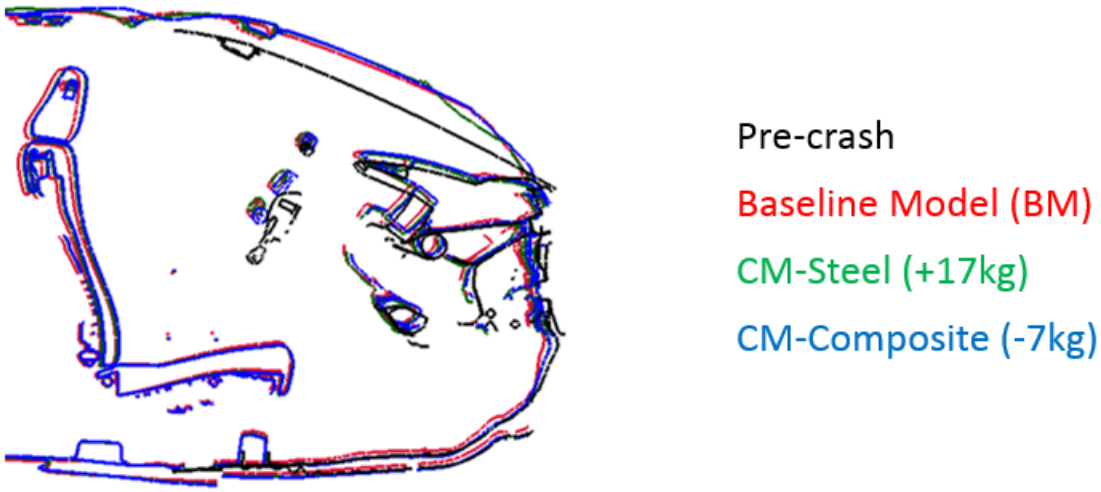

Figure 23 – IIHS Small Overlap – BM vs. CM-Steel and CM-Composite

Figure 24 shows the vehicle pulse, measured at the rear of the vehicle. An overall similar vehicle pulse was observed for the CM-Steel vehicle, shown in green, and the CM-Composite vehicle, shown in blue. The maximum peak of both vehicles was similar to the BM, shown in red. The maximum peak of the BM, CM-Steel vehicle, and CM-Composite vehicle was smaller than for other co-linear impact configurations.

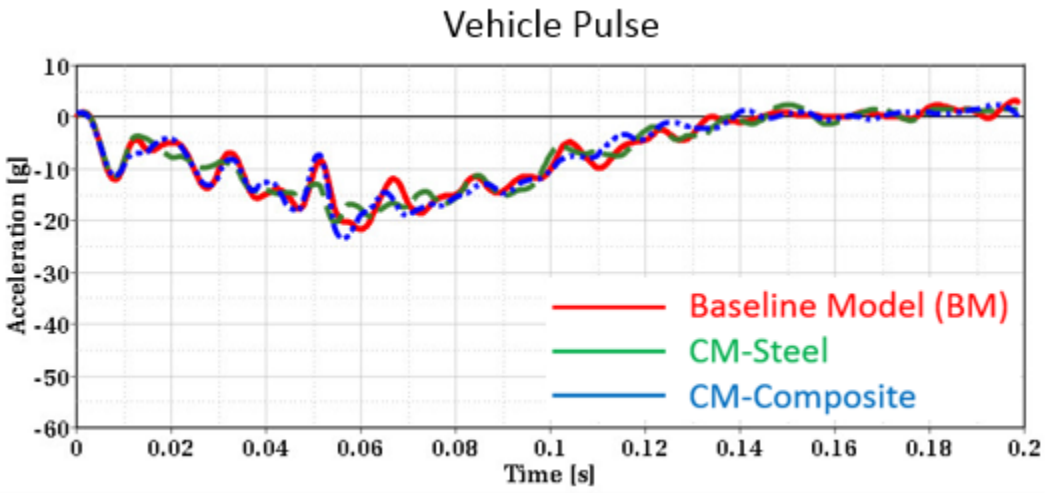

Figure 24 – IIHS SO Vehicle Pulse – BM vs. CM-Steel and CM-Composite

No significant effect with respect to restraint system performance and occupant injury risk due to the introduced structural changes for CM-Steel and CM-Composite was therefore predicted.

4.8. Material Model Development

In an ongoing effort in cooperation with Honda R&D, a shell element version of Material Model MAT_213 in LS-DYNA for simulation of composites is being developed and validated.

Between 2015 and 2018, the National Aeronautics and Space Administration (NASA), the Federal Aviation Administration (FAA), the Arizona State University (ASU), the George Mason University (GMU), and the Ohio State University's (OSU) composite material modeling consortium has sponsored the development of a material law (MAT_213) in the commercial LS-DYNA code for the simulation of composite materials under ballistic loads.

The MAT_213 has some features, such as (1) a deformation model involving elastic and plastic deformations, (2) dependency of strain-rate and temperature, (3) a damage model, (4) a failure model, and (5) a stochastic variation model. The model is driven by tabular data that is generated either using laboratory tests or via virtual testing. However, this material law was implemented for solid elements only.

In cooperation with Honda, GMU is implementing this material law for plane stress conditions so that it can be used by shell elements based on thin shell theory. This will allow to apply the material law to the simulation of thin panels undergoing loads occurring in automotive crash applications.

Current activities includes code development and verification, characterization of a material law for a composite material based on coupon testing, comparison of different discretization techniques when used in conjunction with MAT_213 for solids and/or shells, and validation of the material model based on component testing.

Many coupon tests are required to develop the material parameters of the material model for a particular composite. The developed material model will be validated by component test simulations, such as head form impact test and static/dynamic crush tests.

The material development and validation efforts within the formed consortium is of significant relevance for the research conducted by GMU for ACC. Honda is planning to share this work with plastic and composite material suppliers to allow them to develop material models of their composite products. That way, OEMs can directly use the material models provided from suppliers to be used in crash simulations for component designs and other analyses.

It is anticipated that this new material model will allow to better simulate and predict the crash performance of components made out of composites in the future. Plastic and composite material suppliers can use methods and tools developed by the GMU Team in previous projects to evaluate their components in relevant crash loading conditions.

(BLANK)

5. Conclusion

This research project led to a further understanding of the numerical polymer/composite material models and their CAE applications.

NHTSA found that oblique crashes represent common real-world accident patterns. The risk of injury in oblique impact configurations is often higher than in co-linear crashes. IIHS found that the risk of lower extremity injury was higher in the oblique impact tests compared to small overlap co-linear impact tests. The development of countermeasures for both restraints and vehicle structure for oblique configurations will therefore potentially improve vehicle safety and reduce injury risk in the future. Consequently, NHTSA is considering adopting a frontal oblique impact configuration into its NCAP rating protocol. NHTSA has contracted GMU in a previous project to evaluate structural countermeasures using high-strength steel materials, including associated mass, to reduce occupant compartment intrusion in the oblique impact condition.

A FE model of an appropriate mid-sized passenger vehicle was developed and validated to match the acceleration and intrusion measurements available from full-scale crash tests. Crash mechanisms that specifically contributed to high intrusion in the oblique impact condition were analyzed. Local deformation and buckling of the toe-pan, was found to be mainly responsible for producing high intrusions for both left-side and right-side oblique configurations.

A 60% reduction of the maximum intrusion was defined as the main design goal. Another design goal was to maintain moderate vehicle pulses in all impact configurations as a prerequisite for good restraint system performance and low injury risk in current and future rating tests. A model with a possible set of countermeasures using high-strength steel materials (CM-Steel) was developed. The associated increase in vehicle mass for the CM-Steel vehicle compared to the BM was +17 kg.

In the current project, countermeasures using composite material, i.e. Carbon Fiber Reinforced Plastic (CFRP), were developed to achieve a similar reduction in occupant compartment intrusion (“CM-Composite”). The associated reduction in mass for the CM-Composite was -7 kg compared to the BM and -24kg compared to the CM-Steel vehicle.

The change in vehicle pulse due to the developed countermeasures was not significant for oblique and co-linear impacts. Therefore, no unintended consequences were predicted.

In a parallel effort in cooperation with Honda R&D, a shell element version of Material Model MAT_213 in LS-DYNA for simulation of composites is being developed and validated. This will allow for better simulating and predicting the crash performance of components made out of composites in the future.

(BLANK)

6. References

ACC Plastics Division. (2009a). Plastic and composite intensive vehicles: an innovation platform for achieving national priorities. Available at www.plastics-car.com/pcivs

ACC Plastics Division. (2009b). Retrieved from plastic in automotive markets technology roadmap – a new vision for the road ahead. Available at www.plasticscar.com/roadmap_fullversion

ACC Plastics Division. (2014). Plastics and polymer composites technology roadmap for automotive markets. Available at http://www.plastics-car.com/Tomorrows-Automobiles/Plastics-and-Polymer-Composites-Technology-Roadmap

Barnes, G., Coles, I., Roberts, R., Adams, S. O., Garner, D. M. (2010). Crash safety assurance strategies for future plastic and composite intensive vehicles (PCIVs). (Report No. DOTVNTSC-NHTSA-10-01). Cambridge, MA: Volpe National Transportation Systems Center.

Bean, J., Kahane, C., Mynatt, M., Rudd, R., Rush, C., Wiacek, C., National Highway Traffic Safety Administration, “Fatalities in Frontal Crashes Despite Seat Belts and Air Bags”, DOT HS 811 202, 2009

BMWBLOG. (2017). Webpage accessed by Jan. 3, 2017, Available at http://www.bmwblog.com/2013/08/13/bmw-i8-bmwblog-first-drive/

Brecher, A. (2007, November). A safety roadmap for future plastics and composites intensive vehicles. (Report No. DOT HS 810 863). Washington, DC: National Highway Traffic Safety Administration.

Brecher, A., Brewer, J., Summers, S., & Patel S. (2009). Characterizing and enhancing the safety of future plastic and composite intensive vehicles. 21st International Conference on the Enhanced Safety of Vehicles, Stuttgart, Germany.

Calspan Corporation, Report for Frontal Oblique Offset Program Testing of a 2012 Toyota Camry, NHTSA No.: R&D-CAL-12-005, Buffalo, USA, 2013

Calspan Corporation, Report for Frontal Oblique Offset Program Testing of a 2012 Toyota Camry, NHTSA No.: R&D-CAL-12-002, Buffalo, NY, USA, 2013

Calspan Corporation, Report for Frontal Oblique Offset Program Testing of a 2014.5 Toyota Camry, NHTSA No.: R&D-CAL-14-005, Buffalo, USA, 2015

DOT / NHTSA, Federal Register Vol. 80 No. 241, New Car Assessment Program (NCAP), Request for comments, December 2015

DOT / NHTSA, Oblique Test Procedure - Draft 7-22-2015, NHTSA-2015-0119-0017, https://www.regulations.gov/document?D=NHTSA-2015-0119-0017

DOT/NHTSA, Docket No. Federal Register Vol. 80 No. 241, New Car Assessment Program (NCAP), Request for comments, January 2017

ExtremeTech. (2017). Webpage accessed by Jan. 3, 2017, Available at https://www.extremetech.com/extreme/209812-how-bmw-weaves-bakes-and-builds-the-carbon-fiber-7-series

Fisher, M., & Cundiff, B. (2002). APC vision and technology roadmap for the automotive market-defining priority research for plastics in 21st century vehicles. (SAE Technical Paper 2002-01-1890). Warrendale, PA: Society of Automotive Engineers.

Fisher, M., Kolb, J., & Cole, S. (2007). Enhancing future automotive safety with plastics. (Paper Number 07-0451). 20th International Conference on the Enhanced Safety of Vehicles, Lyon, France.

Hallquist, J.O., "LS-DYNA Keyword User Manual, Livermore Software Technology Corporation, February 2013

Hollowell, W.T., Gabler, H.C., Stukci, S.L., Summers, S., Hackney, J.R. (1998). Review of potential test procedures for FMVSS No. 208, Office of Vehicle Safety Research.

IIHS, 2015 Toyota Camry (CEN1349) Small Overlap Frontal Test, Arlington, USA, 2013

Jäschke, A., Dajek, U. (2004). Roof-frame design using hybrid technology. VDI-Report No. 4261, pages 25 – 45. Available at https://techcenter.lanxess.com/scp/emea/en/docguard/Roof-frame_design_using_hybrid_technology.pdf?docId=63459

LANXESS. (2007). Case Study: body reinforcement using CORE products CBS technology with carriers made of Durethan® BKV 35. Available at https://techcenter.lanxess.com/scp/emea/en/docguard/TI_2006-048_EN_Case_D_BKV_35_CORE_-_body_reinforcement.pdf?docId=5418726

Marzougui, D., Brown, D., Park, C-K., Kan, C.D., Opiela, K.S. (2014). Development & validation of a finite element model for a mid-sized passengers Sedan. Presented at the 13th International LS-DYNA Users Conference, USA, June 8–10, 2014

Mueller, R., "Comparison of frontal crash modes: IIHS small overlap and NHTSA oblique", Insurance Institute for Highway Safety, SAE Government/Industry Meeting, Washington, DC, 2017

Park, C-K., Kan, C-D., Hollowell, W., & Hill, S.I. (2012, December). Investigation of opportunities for lightweight vehicles using advanced plastics and composites. (Report No. DOT HS 811 692). Washington, DC: National Highway Traffic Safety Administration. Available at www.nhtsa.gov/DOT/NHTSA/NVS/Crashworthiness/Plastics/811692.pdf

Park, C-K., Kan, C-D., Hollowell, W. (2013). Investigation of crashworthiness of structural composite components in frontal and side NCAP tests. SAE Technical Paper, 2013-01-0650, 2013; SAE World Congress & Exhibition, Detroit, MI, USA, April 16-18, 2013.

Park, C-K., Achstetter, T., Kan, C-D., Hollowell, W. (2017). "Understanding of Numerical Polymer/Composite Material Models and Their CAE applications", Final Report.

Reichert, R., Mohan, P., Marzougui, D., Kan, C.D., Brown, D. (2016). Validation of a Toyota Camry finite element model for multiple impact configurations. SAE Technical Paper 2016–01–1534, 2016, doi:10.4271/2016-01-1534

Reichert, R., Kan, S.: "Development of a 2015 Mid-Size Sedan Vehicle Model", 11th European LS-DYNA Conference 2017, Salzburg, Austria.

SAE International website, "Camry's Mid-Cycle 'Refresh' More Than Just Front and Rear Panels". http://www.articles.sae.org/13135, accessed September 7, 2016

Saunders, J., Craig, M.J., Suway, J., "NHTSA's Test Procedure Evaluations for Small Overlap/Oblique Crashes," The 22nd International Technical Conference for the Enhanced Safety of Vehicles, Paper No. 11-0343, 2011

Senate. (2007). Transportation, treasury, housing and urban development, the judiciary, and related agencies appropriations bill. Report (to Accompany H.R. 5576), Issues 109-293, Page 62, Available at https://www.congress.gov/109/crpt/srpt293/CRPT-109srpt293.pdf

Skszek, T. (2015, December). Demonstration project for a multi-material lightweight prototype vehicle as part of the clean energy dialogue with Canada. Final Report Summary. Available at https://www.osti.gov/scitech/biblio/1332277-demonstration-project-multi-material-lightweight-prototype-vehicle-part-clean-energy-dialogue-canada

Takefumi Shiga, (2014) "Challenge for light weight", CAR Management Briefing Seminars 2014, August 4–7, 2014, Available at http://www.cargroup.org/?module=Schedule&confID=6&event=Session&sessionID=43

Tetex. (2017).Webpage accessed by Jan. 3, 2017, Available at http://www.tetex.com/carbon-fiber-at-hyundai-andbmw/

The Truth About Cars. (2017). Webpage accessed by Jan. 3, 2017, Available at http://www.thetruthaboutcars.com/2012/07/the-making-of-the-lexus-lfa-supercar-an-inside-report-chapter-3-call-me-names/#more-452054

Thunert, C., "CORA Release 3.6 User's Manual," Version 3.6, GNS mbH, Partnership for Dummy Technology and Biomechanics (PDB), 2012

Volpe National Transportation Systems Center. (2008). A summary of proceedings for the safety characterization of future plastic and composite intensive vehicles (PCIVs). Cambridge, MA: Author. Available at http://ntl.bts.gov/lib/32000/32200/32205/summary_pciv_workshop.pdf.

Zhang, R., Reichert, R., Kan, C.-D. and Cao, L. "Evaluation of driver lower extremity injuries in 16 oblique crashes with THOR", International Journal of Crashworthiness, 2015, doi: 10.1080/13588265.2015.1120983

(BLANK)

7. Appendix

A1 – Mass and Cost Analysis BM and CM-Steel

		Baseline Model (BM)					
Part		Yield Strength {Mpa]	Assumed Grade	Gauge [mm]	Mass [kg]	Price [$/kg]	Cost [$] Based on 65%
Firewall		250	BH 260/370	2.1	19.6	0.91	27.44
Hinge Pillar (a)		360	DP 350/600	0.9	0.9	1.16	1.61
Hinge Pillar (b)		360	DP 350/600	1.1	1.5	1.16	2.68
Hinge Pillar (c)		360	DP 350/600	1.3	1.2	1.16	2.14
Front Rail (a)*		360	DP 350/600	2.8	4.3	1.16	7.67
Front Rail (b)*		360	DP 350/600	2.1	4.2	1.16	7.5
Mid-Rail (a)*		360	DP 350/600	1.6	3.7	1.16	6.6
Mid-Rail (b)*		360	DP 350/600	1.4	2.4	1.16	4.28
Mid-Rail (c)*		360	DP 350/600	2	9.4	1.16	16.78
* left and right side combined							

		Countermeasure Model 2 (CM2)							Delta	
Part		Yield Strength {Mpa]	Assumed Grade	Gauge [mm]	Mass [kg]	Price [$/kg]	Cost [$] Based on 65%		Δ Cost [$]	Δ Mass [kg]
Firewall		360	DP 350/600	3.2	29.8	1.16	53.18		25.74	10.2
Hinge Pillar (a)		450	DP 500/800	1.4	1.4	1.21	2.61		1	0.5
Hinge Pillar (b)		450	DP 500/800	1.6	2.2	1.21	4.1		1.42	0.7
Hinge Pillar (c)		360	DP 350/600	1.8	1.7	1.16	3.03		0.89	0.5
Front Rail (a)*		360	DP 350/600	2.1	3.6	1.16	6.42		-1.25	-0.7
Front Rail (b)*		360	DP 350/600	1.8	3.4	1.16	6.07		-1.43	-0.8
Mid-Rail (a)*		450	DP 500/800	2.4	5.5	1.21	10.24		3.64	1.8
Mid-Rail (b)*		450	DP 500/800	2.2	3.7	1.21	6.89		2.61	1.3
Mid-Rail (c)*		360	DP 350/600	2.8	13.2	1.16	23.56		6.78	3.8
* left and right side combined							**Total**		**39.4**	**17.3**

The total change in mass for CM2 was +17.3 kg. The total change in cost for CM-Steel was +$39.40.

A2 – Left Oblique - Firewall Deformed Shape

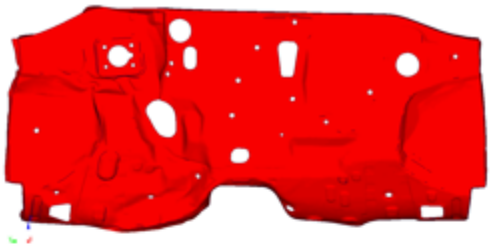

BM-Steel

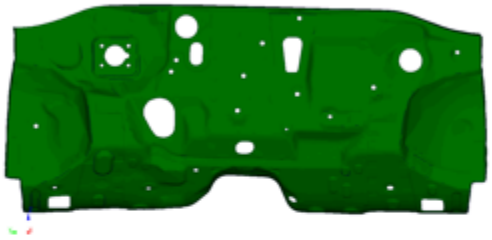

CM-Steel (+17kg)

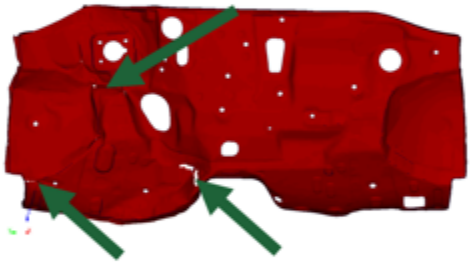

CM-Composite 1
(1.2mm, -15kg)

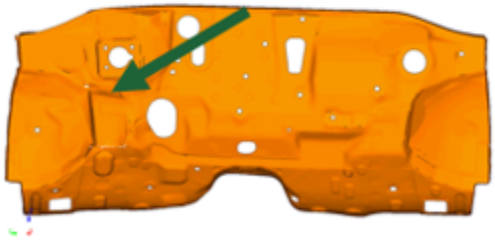

CM-Composite 2
(2.4mm, -11kg)

CM-Composite 3
(3.6mm, -7kg)

A3 – Left Oblique – Vehicle Pulses

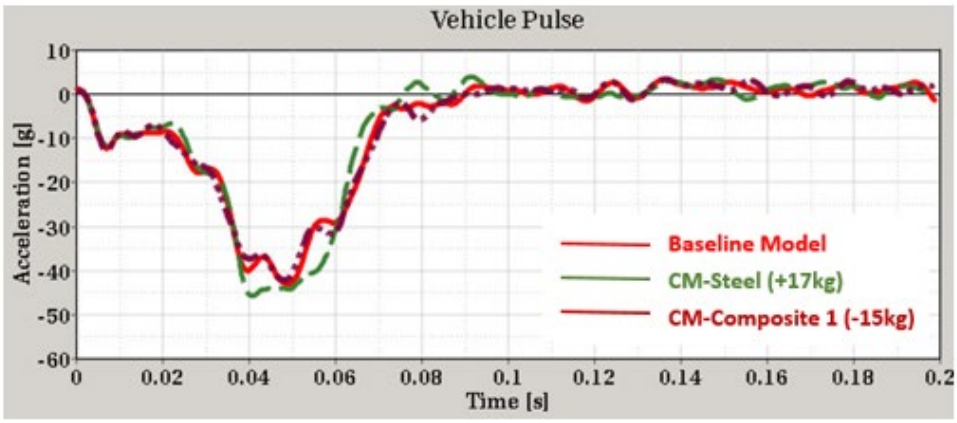

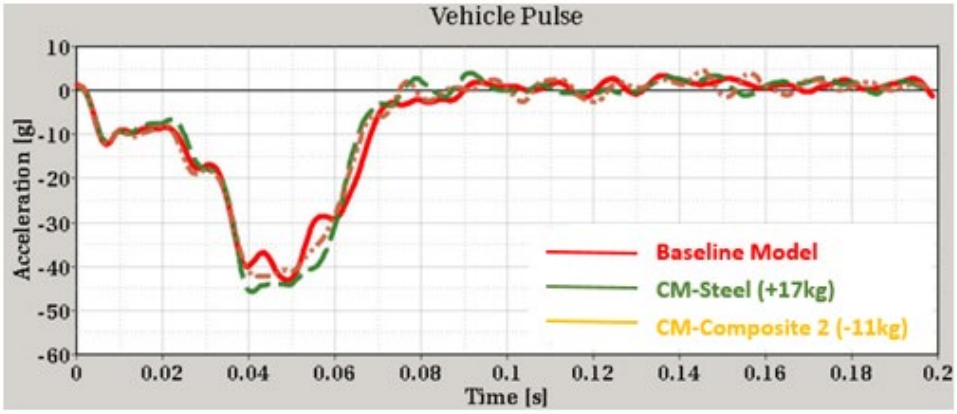

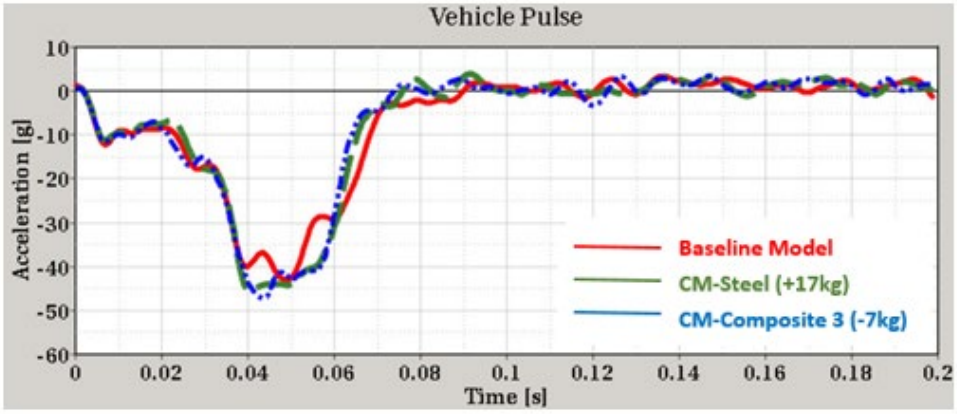

A4 – Right Oblique – Firewall Deformed Shape

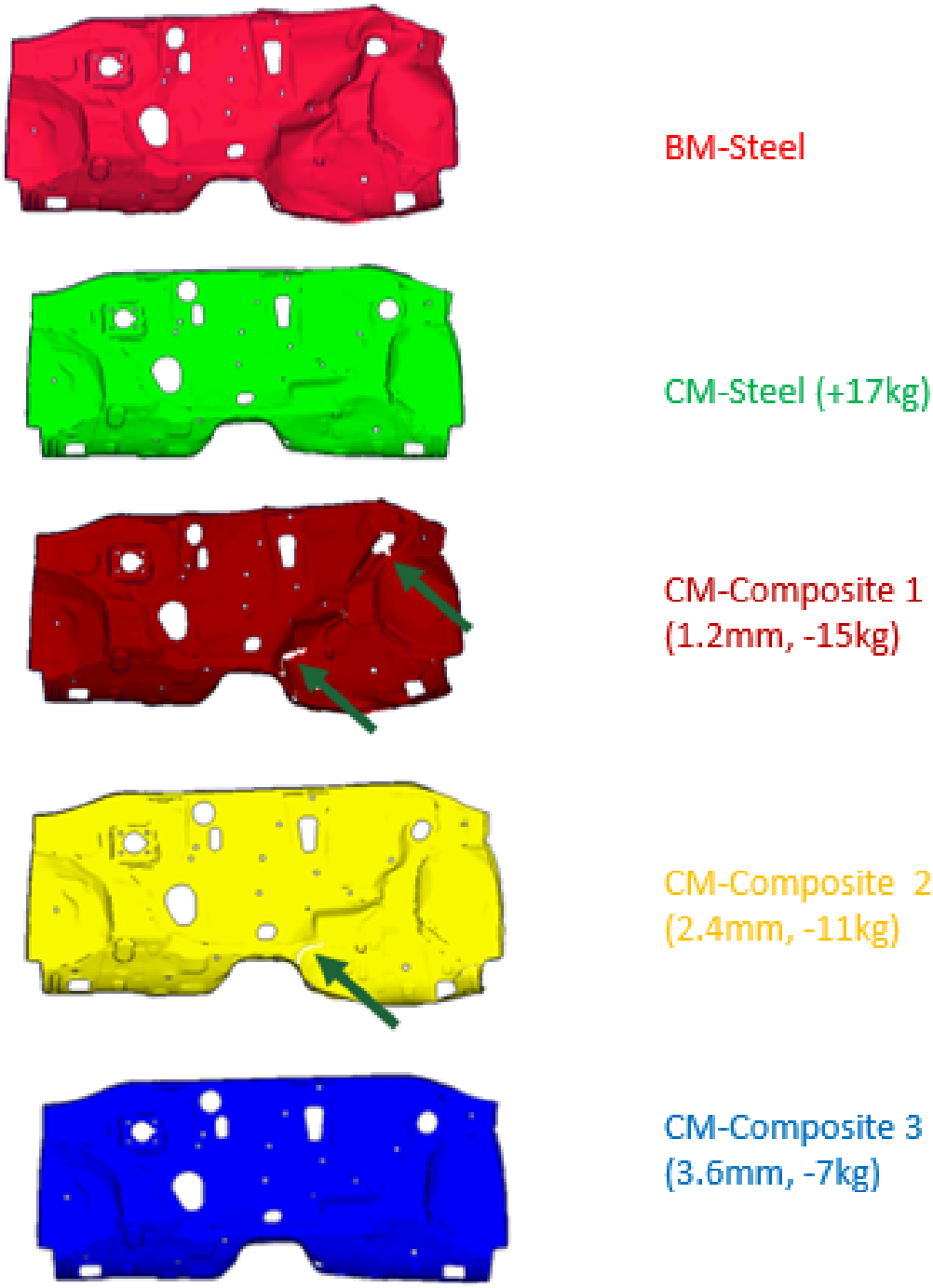

A5 – Right Oblique – Vehicle Pulses

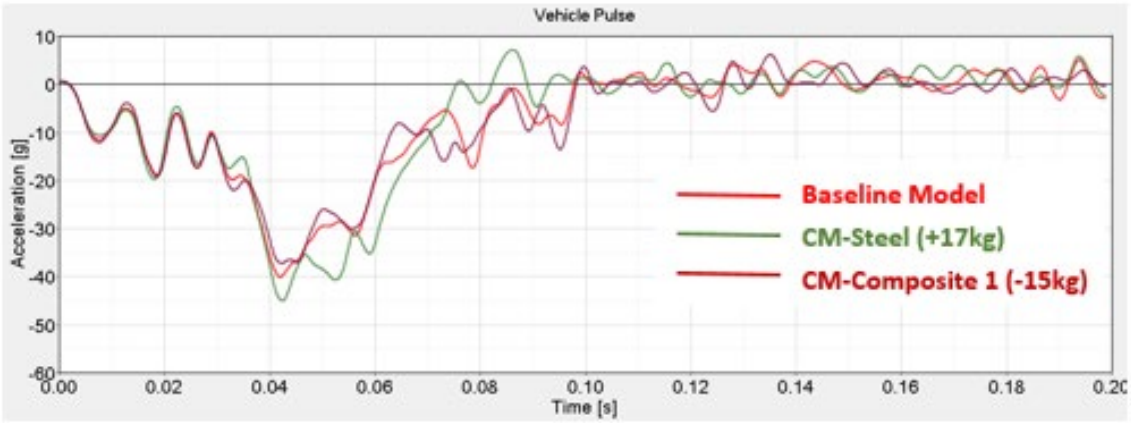

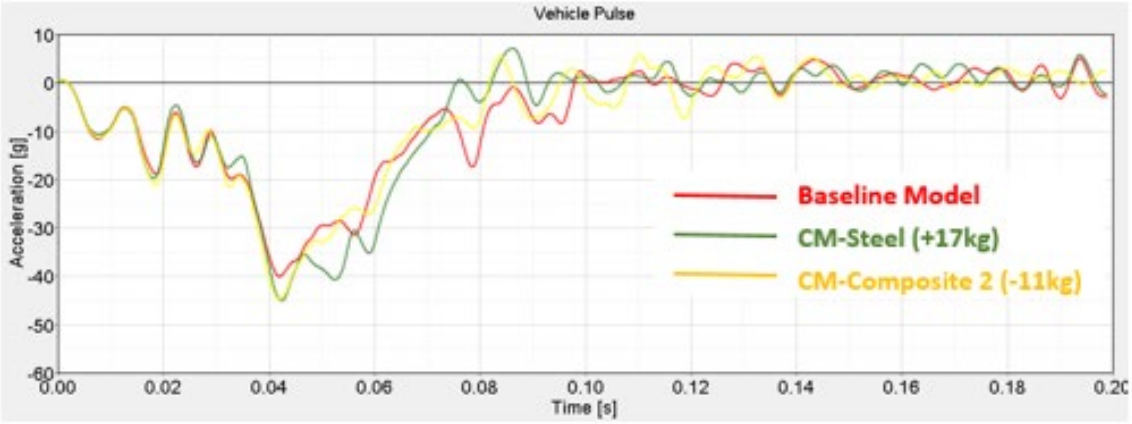

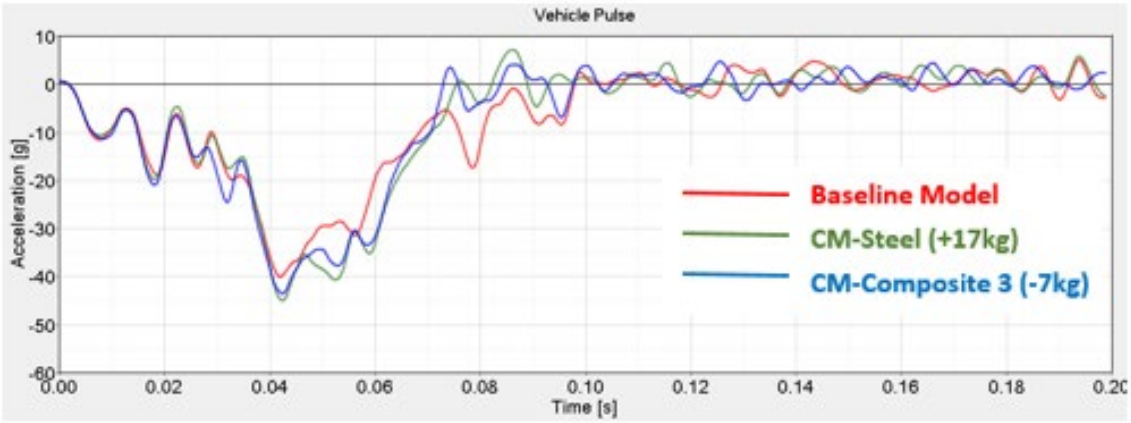

(BLANK)